

University of Southern Queensland
Faculty of Health, Engineering and Sciences

Numerical and Physical Modelling of a 2D Tunnel Heading at Collapse

A dissertation submitted by

Mathew Steven Sams

In fulfilment of the requirements of

Courses ENG4111 and ENG4112 Research Project

towards the degree of

Bachelor of Engineering (CIVIL)

Submitted: October, 2013

Abstract

Predicting surface and sub-surface movement upon tunnel heading failure is essential for safety and contingency planning. This paper presents the results of a 2D physical and numerical modelling experiment of tunnel heading failure in cohesionless soil. By modelling six overburden to diameter ratios, the research seeks to investigate the behaviour, magnitude and failure mechanism of a tunnel heading. The physical model uses displacement control to simulate tunnel heading movement. The use of transparent faced modelling containers allows video capture of the soil movement as the tunnel heading is displaced. From the captured video, Particle Image Velocimetry (PIV) was then utilised to analyse soil movement. This then allowed close monitoring of the soil movement, which allows verification of settlement results and examination of failure behaviour. Numerical modelling using FLAC with FISH programming was then used for further comparison. This research concurred with past tunneling research that suggested a two stage failure mechanism, this is observable from the PIV and FLAC results. It is concluded that the current experimental and numerical procedures produce qualitative results that can be used to compare with results obtained from other research papers of the same area in the future.

University of Southern Queensland
Faculty of Health, Engineering and Sciences

<p>ENG4111 Research Project Part 1 & ENG4112 Research Project Part 2</p>

Limitations of Use

The Council of the University of Southern Queensland, its Faculty of Health, Engineering and Sciences, and the staff of the University of Southern Queensland, do not accept any responsibility for the truth, accuracy or completeness of material contained within or associated with this dissertation.

Persons using all or any part of this material do so at their own risk, and not at the risk of the Council of the University of Southern Queensland, its Faculty of Health, Engineering and Sciences or the staff of the University of Southern Queensland.

This dissertation reports an educational exercise and has no purpose or validity beyond this exercise. The sole purpose of the course "Project and Dissertation" is to contribute to the overall education within the student's chosen degree programme. This document, the associated hardware, software, drawings, and other material set out in the associated appendices should not be used for any other purpose: if they are so used, it is entirely at the risk of the user.

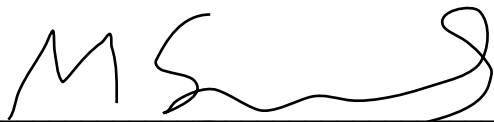
Certification

I certify that the ideas, designs and experimental work, results, analyses and conclusions set out in this dissertation are entirely my own effort, except where otherwise indicated and acknowledged.

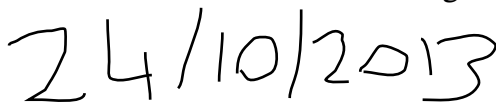
I further certify that the work is original and has not been previously submitted for assessment in any other course of institution, except where specifically stated.

Mathew Sams

Student Number: 0050056349

A handwritten signature in black ink, appearing to read 'MS' followed by a stylized, flowing line that ends in a loop.

Signature

A handwritten date in black ink, written as '24/10/2013'.

Date

Acknowledgements

I would like to thank Dr. Jim Shiau for his time and assistance in the experimentation and with the equipment. As well as this, he provided the FLAC script file that was used in the numerical modelling. Throughout this research he has provided suggestions about the best means to formatting particular aspects of the images.

Thanks must also go to Ryan Kemp for providing some assistance and guidance when possible.

Perhaps the most important thank you is to Dr. David White and Dr. Andrew Take for permitting the use of GeoPIV in this research.

Table of Contents

Abstract	ii
Limitations of Use	iii
Certification	iv
Acknowledgements	v
Table of Contents	vi
List of Figures	ix

1 Project Introduction	1-1
1.1 Background	1-1
1.2 Scope of Work	1-2
1.3 Organisation of Thesis	1-3

2 General Review	2-1
2.1 Introduction	2-1
2.1 Shield Tunneling in Soft Ground	2-1
2.2.1 Process	2-3
2.2.2 Stability	2-4
2.2.3 Soil Movement	2-5
2.3 Physical Modelling	2-6
2.4 Particle Image Velocimetry	2-11
2.5 Numerical Modelling	2-14

3 Physical Modelling	3-1
3.1 Introduction	3-1
3.2 Setup and test material	3-2
3.4.1 Sandbox and Tunnel Model	3-3
3.4.1 Sand Properties	3-4
3.3 Test Procedure	3-6
3.4 Results	3-7

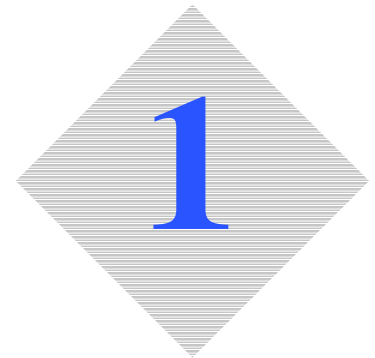
3.4	Conclusions and Recommendations	3-9
4	Particle Image Velocimetry	4-1
4.1	Introduction	4-1
4.2	Equipment and Setup	4-2
4.2.2	Recommendations for future use	4-4
4.3	Procedure of Analysis	4-5
4.4	Results	4-8
4.4.1	Failure behaviour	4-10
4.5	Conclusions and Recommendations	4-11
5	Numerical Modelling	5-1
5.1	Introduction	5-1
5.2	Model Setup	5-2
5.2.1	Statement of Problem	5-2
5.2.2	Setuip and Parameters	5-3
5.3	Results	5-5
5.4	Conclusions and Recommendations	5-8
6	Conclusions	6-1
7.1	Summary	6-1
7.2	Future Work and Closing Comments	6-2
7	References	7-1
8	Appendices	8-1
9.1	Appendix A – Project Specification	8-1
9.2	Appendix B – Output script for PIV results	8-3
9.3	Appendix C – Extra Reference Material	8-4

List of Figures

Figure 2-1 Tunnel Boring machine (Herrenknecht)	2-2
Figure 2-2 Example of an EPB tunnel boring machine (Herrenknecht) ..	2-3
Figure 2-3 Comparison of predictions of heading pressure in sand (Kirsch A, 2009)	2-4
Figure 2-4 Gaussian model for settlement	2-5
Figure 2-5 Models used by Kirsch, 2010	2-6
Figure 2-6 Results from Kirsch, 2010	2-7
Figure 2-7 Diagram of physical model Chen et al, 2013.	2-7
Figure 2-8 Heading pressure and settlement results from Chen et al, 2013	2-8
Figure 2-9 Pressure distribution under a pile of soil, Smid and Novosad, 1981	2-9
Figure 2-10 Model used in Ahmed and Iskander, 2012	2-9
Figure 2-11 Heading pressure and diaplacment results from Ahmed and Iskander, 2012	2-10
Figure 2-12 PIV being used to analyze flow path of a creek (jPIV, 2013)l	2-11
Figure 2-13 Resolution versus Precision (White and take, 2003)	2-13
Figure 2-14 Patch size versus precision error (White and Take, 2003) ..	2-13
Figure 2-15 PIV results from Kirsch, 2010	2-14
Figure 2-16 3D model and results from Kirsh, 2010 using ABAQUS	2-15
Figure 2-17 Results and mesh used from Wong et al, 2012	2-16
Figure 2-18 Mesh and results from FLAC analysis (Ohta and Kiya, 2001)	2-16
Figure 3-1 Geotechnical centrifuge (Columbia University, 2005)	3-2
Figure 3-2 Soil sample and model tunnel at the start of the test	3-3
Figure 3-3 Front view of model	3-4
Figure 3-4 Apparatus used in a Direct shear test (left), diagram of the core mechanism (right)	3-5
Figure 3-5 Results of shear box test on the sand	3-6
Figure 3-6 Measured settlement parameters	3-7
Figure 3-7 Results for Smax	3-8
Figure 3-8 Results for B	3-8
Figure 3-9 Results for L	3-9
Figure 4-1 Setup of camera	4-2
Figure 4-2 Zone of interest in the PIV analysis	4-3
Figure 4-3 Wild Vectors in the PIV analysis	4-4
Figure 4-4 Mesh generation in geoPIV	4-5
Figure 4-5 Examples of mesh and element files created by geoPIV	4-6
Figure 4-6 Example of geoPIV launcher file	4-7
Figure 4-7 PIV vector plots for C/D 2-3 (left to right)	4-8
Figure 4-8 PIV vector plots for C/D 4-7 (left to right)	4-9
Figure 4-9 C/D=5 case, with PIV plots for 1/4, 1/2, 3/4 and full heading retraction time	4-10

Figure 5-1	Ideal model of system	5-2
Figure 5-2	Screenshot of a portion of the FLAC script being used	5-3
Figure 5-3	Typical mesh in FLAC	5-4
Figure 5-4	Heading pressure and displacement for the six C/D cases ..	5-5
Figure 5-5	Example history plot of unbalanced forces of C/D=4	5-6
Figure 5-6	Comparison of PIV plot and FLAC velocity plot in the C/D=4 case	5-6
Figure 5-7	Comparison of PIV plot and FLAC strain rate plot for the C/D=4 case.	5-7
Figure 5-8	Failure plots showing the failure pattern (showing 50%, 80%, 90%, 100% relaxation)	5-7
Table 3-1	Results From density test	3-5

Introduction



1.1 Background

Modern cities and highly developed regions around the world are struggling to cope with increased motor vehicle traffic. There have been many methods for coping, such as public transport, and inner city tolls. These methods have been met with limited success, but there is still a strong need for inner city roads. However, space for expansion and/or upgrading of such infrastructure is generally limited can cause significant public disruption. Because of this, tunneling is increasingly becoming a preferred solution because of the safety, economic, and engineering advancements of tunnel boring machines (TBM). Locations where tunneling was once considered not viable due to sensitivity to ground movement or geological complexity are now possible due to these advances.

Even though these tunneling machines are now relatively safe and reliable, it is still essential to be aware of the surface movement should the tunnel heading collapse. Cohesionless sand has a tendency to fail under its own weight if tunnel heading stability is not maintained. Therefore, estimation and control of face pressures and ground movement is essential to minimize impact on nearby structures. Tunneling technology has significantly advanced in the past few decades . However, engineers are often relying on empirical and theoretical methods for this which are based on limited field testing (Meguid et al, 2008). Such methods include design charts and numerical methods. Whilst these may give accurate predictions under some circumstances, the validity of such analyses should be verified with modelling (Chen at al, 2013).

Numerical and physical modelling in two and three dimensions is increasingly being used to give reliable results over a wider range of scenarios. Physical modelling is done most commonly using small scale tanks (Messerli et al, 2010; Kirsch, 2009; Vardoulakis, 2009), which are relatively easy to construct and give a good representation of reality. Particle

Image Velocimetry is an effective way of displaying the movement of particles in physical modelling. Software for this is widely available, and has been in development for long enough that it can be completed with relative ease, and is now quite commonly used in geotechnical research. Numerical modelling is done using the commercially available FLAC in most circumstances. This is a powerful tool that can be used to model any number of scenarios in a relatively short period of time because of significant computing advances in the last 10 years. This project will model a tunnel heading collapse at various depths using both small scale physical models with particle image velocimetry and also FLAC numerical modelling, to demonstrate soil movement phenomenon and heading instability.

1.2 Scope of Work

The purpose of this research is to investigate tunnel heading stability and soil movement upon collapse in cohesionless soil over a range of cover to diameter ratios (C/D). In this case, the range will be 2–7. To do this, several methods will be used: physical modelling using scale models with a transparent face, particle image velocimetry (PIV) to demonstrate the movement of the soil in these models, and numerical modelling using FLAC2D software. The sand used will be kept constant and the properties of this sand will then be used in the numerical modelling. In addition to this, the material being focussed on in this project is sand, and sand only.

The modelling will only be two-dimensional in this project, as the increased complexity, time and cost of doing three-dimensional was considered unnecessary in this particular case. It should be noted that modelling this particular problem in 2D is considered conservative, as the effects of the soil structure in the other axis are being disregarded.

1.3 Organisation of Thesis

Chapter 2 - General Review: Chapter 2 presents a review of the tunnelling process and explains some concepts relating to tunnelling. A review of the current literature is also included in this section. Physical modelling of tunnel stability in sand using scale models, numerical modelling of tunnel stability using FLAC software, and Particle Image Velocimetry (PIV) are all reviewed. A brief introduction to PIV and FLAC is also given.

Chapter 3 - Physical Modelling: Discuss the design and operation procedure of the tanks. Then the results of this modelling will be presented.

Chapter 4 - Particle Image Velocimetry: This chapter will discuss and introduce the technique of Particle Image Velocimetry. The variety of software available, and the reasoning for the selection of the used software will be addressed. Operational procedure will be explained with detail on configuration and setup parameters. Lastly, some results will be presented with some discussion and comparison with the numerical modelling and previous research.

Chapter 5 - Numerical Modelling: This chapter begins with an introduction to FLAC software, in which the selection of this software is addressed. The script to be used in the analyses is covered, and then results will be presented appropriately with discussion.

Chapter 6 - Conclusions: This section will include a short summary of what has been achieved in this research project, some key outcomes that have been reached, and also some recommendations on further work to be done from this research.

General Review



2.1 Introduction

Predicting surface and sub-surface movement upon tunnel heading failure is essential for safety and contingency planning. This paper presents the results of a 2D physical modelling experiment of tunnel heading failure in cohesionless soil. By modelling six overburden to diameter ratios, the research seeks to investigate the behaviour, magnitude and failure mechanism of a tunnel heading. The physical model uses displacement control to simulate tunnel heading movement. The use of transparent faced modelling containers allows video capture of the soil movement as the tunnel heading is displaced. This then allowed close monitoring soil movement, which allows verification of settlement results and examination of failure behaviour. It is concluded that the current experimental procedures produce qualitative results that can be used to compare with results obtained from numerical experiments carried out using FLAC software.

In order to successfully fulfil the aims of this project some knowledge of the subject area is required, and that is what will follow.

2.2 Shield Tunneling in Soft Ground

Tunneling is a concept that has existed for a long time, but the ability for them to be engineered safely and reliably has only been able to happen in relatively recent times. This is caused by an increase in research and development in tunneling technology, brought about by the need to satisfy the demand for infrastructure alternatives to bridges and cross-city highways, and also to traverse mountain ranges.

Most tunneling projects around the world now use tunnel boring machines (TBM), of which there are two main types. The first is the Earth Pressure Balance (EPB) TBM which is used in cohesive soils like clay. This is the most common and is very adaptable to different ground conditions. The second is the slurry tunneling machines (STM), which are most commonly used in unstable soils without cohesion like dry sand, or liquid soils, although even modern EPB's are capable of being used in these conditions. In both mechanisms an internal pressure is generated to support the cutting face against the existing overburden and hydrostatic pressures (Ahmed and Iskander, 2012).



Figure 2-1. Tunnel Boring machine (Herrenknecht)

The size of tunnels that can be constructed using TBM is wide ranging, and can be micro tunnels used for pipes and cabling (Jebelli et al, 2010), up to three lane highways such as the 19.25m Orlovski tunnel in St Petersburg, such as the one shown in figure 2-1.

2.2.1 Process

TBM's can be as long as 100 metres, depending on the size and complexity of the tunnel, and they can be broken into three main parts: the cutting face which slowly rotates and is pushed into the tunnel face by hydraulic jacks, the soil extraction area where the cut soil is extracted from behind the cutting face, and the transport and operations area where the cut soil is transported out of the tunnel and the operational staff monitor the machine. An image showing the layout of a typical tunnel boring machine is shown below in figure 2-2.



Figure 2-2. Example of an EPB tunnel boring machine (Herrenknecht)

Pressure at the cutting face is very critical and is kept within strict limits. Heading pressure that is too low will cause a local soil failure at the tunnel heading area, or perhaps a global failure in extreme cases. On the other hand, heading pressure that is too high will result in soil being pushed away from the cutting face, rather than being cut and excavated which may cause excess compressive stress on the above soil, and in extreme cases, blowout at the surface.

2.2.2 Stability

Tunnel heading stability refers to the problem described immediately above, where the need to govern the pressure applied to the cutting face absolutely critical. Heading stability is the problem, and methods to predict the required pressure still vary significantly between various methods and research results. This problem is widely debated amongst tunneling researchers and is the basis of most tunneling research at the moment. Maintaining heading stability requires predicting the required pressure that the hydraulic jacks or the slurry need to apply to the heading to avoid soil failure. A number of authors have described failure mechanisms at the tunnel face, and have derived formulae to calculate the appropriate face support pressure based on the limit equilibrium method (e.g. Davis et al., 1980; Leca and Dormieux, 1990; Lee and Nam, 2001; Li et al., 2009; Mollon et al., 2009, 2010; Horn, 1961). Methods for predicting this required support pressure are somewhat lacking and can be inconsistent. (Ahmed and Iskander, 2012 and Kirsch A, 2009).

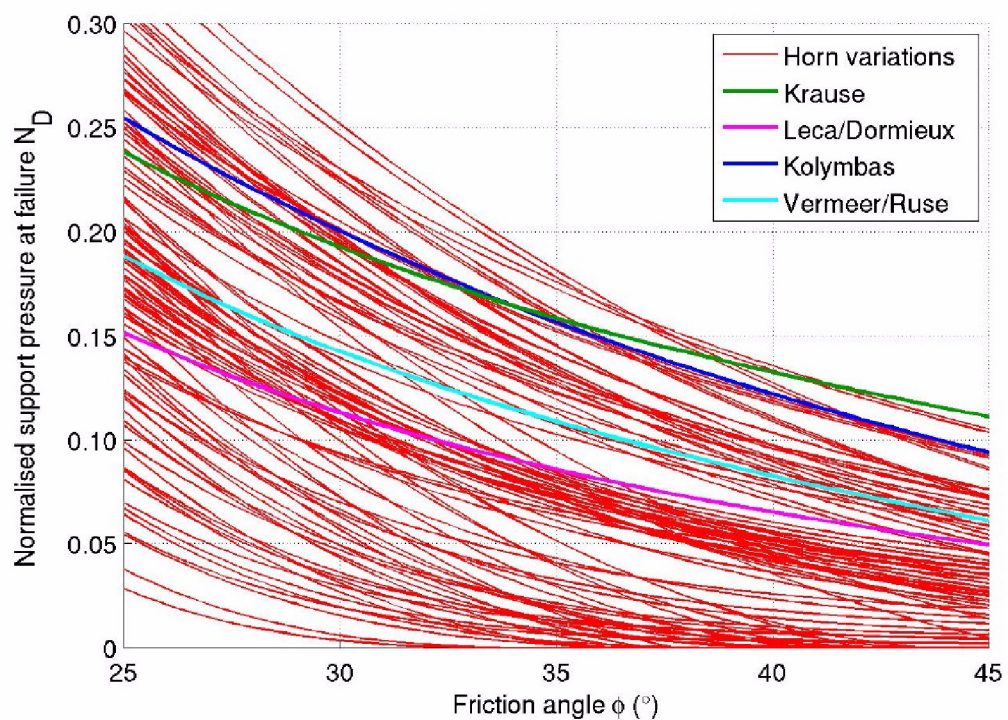


Figure 2-3. Comparison of predictions of heading pressure in sand (Kirsch A, 2009)

This inconsistency is well illustrated in figure 2-3, where only the friction angle is being varied. Predicting heading pressure with varying C/D further complicates the process.

2.2.3 Soil Movement

Minimizing soil movement is very critical when using a TBM. Even slight soil movement at the surface can cause damage to buildings and infrastructure. Controlling heading pressure is the best way to limit soil movement, and stop local soil failures. The use of improved TBM technology and construction techniques means that tunneling in more difficult ground condition within settlement sensitive (i.e. urban) areas are increasingly being considered and undertaken. Tunneling induced surface settlement is a complex phenomenon that is dependent on soil and groundwater conditions, tunneling dimensions and construction techniques (Lee, Rowe & Lo 1992). Thus, being able to accurately predict surface settlement for safety and contingency planning reasons is very important.

The theoretical and empirical methods for predicting settlement profile basically all assume a gaussian curve for the profile, which was introduced by Peck in 1969. His formula for settlement was:

$$S_x = (AV_L/2.5i)e^{-x^2/2i^2}$$

Where A is the tunnel area, VL the percentage volume loss, i the trough parameter given by $i=Kz_0$ where K is generally taken as 0.5 (Osman, J & D 2006) but can be up to 0.7 for soft clays. The volume loss (VL) is given by $VS=AVL$ where VL is the volume percentage loss. Figure 2-4 shows this model for settlement.

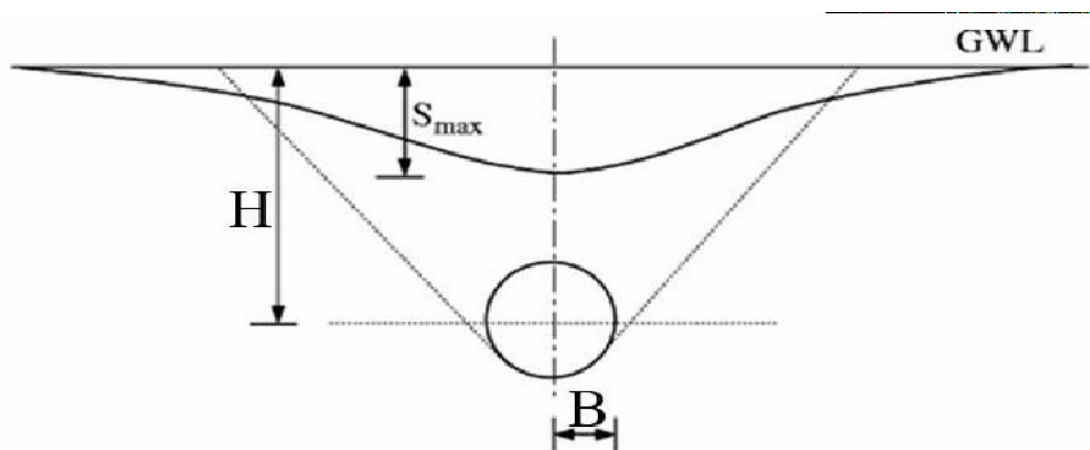


Figure 2-4. Gaussian model for settlement

Osman et al (2006) suggested improvements to this formula. However, with the rapid development of computers in the last 15 years, numerical finite element method modelling

has become the preferred tool for modelling soil movement, in particular soil response to tunneling.

2.3 Physical Modelling

Geotechnical problems in reality are very difficult to model with 100% accuracy because of the number of variables involved, and the number of particular cases where either the material properties or the geometry of the scenario is different. Although numerical modelling has significantly improved in quality and quantity over the last 15 years, it is still somewhat bound by these restrictions. This combined with the need for numerical modelling to be verified means that physical modelling is still a large part of geotechnical research.

However, physical modelling in clay requires the usage of a centrifuge. Several centrifuge model tests have been performed to investigate tunnel face stability (Atkinson et al., 1977; Mair, 1979; Kimura and Mair, 1981; Chambon and Corté, 1994; Al Hallak et al., 2000; Kamata and Mashimo, 2003; Plekkenpol et al., 2006; Meguid et al., 2008; Idinger et al., 2011). These focussed on settlement and heading pressure.

However, as this project is using sand and not clay it is somewhat simpler to do as it does not require using a centrifuge to fail the soil, and the models only need to be relatively simple to give good results. Physical modelling when the material of interest is sand, is still very popular for these very reasons. Kirsch (2010) investigated the failure mechanisms and the evolution of support pressure in dense and loose sands by using two small-scale model tanks with a 10 cm diameter tunnel. This is shown below in figure 2-5.

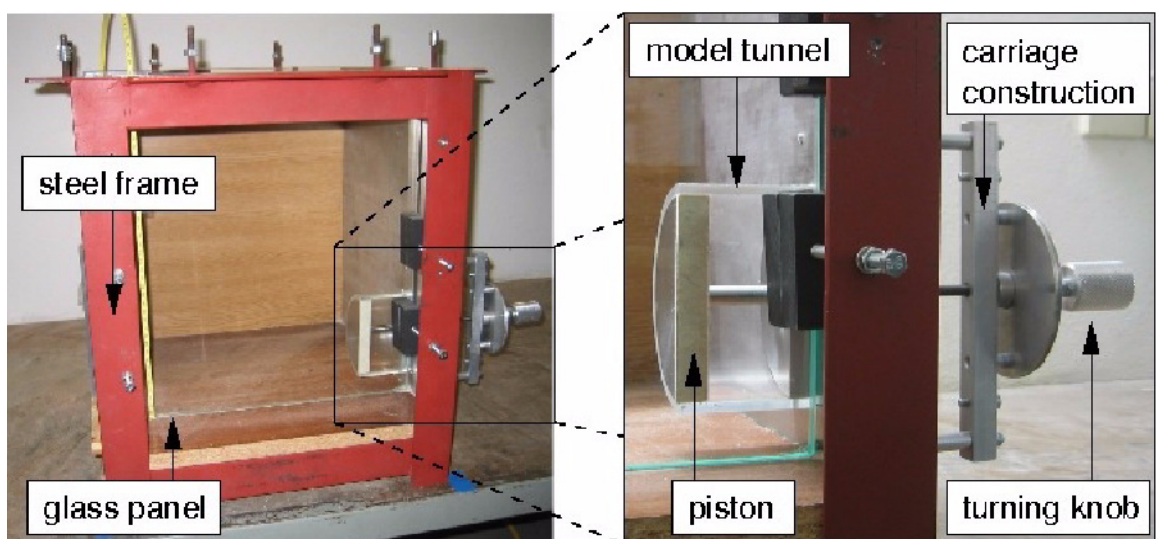


Figure 2-5. Models used by Kirsch, 2010

Kirsch did a total of 52 tests investigating the effects of the friction angle of the sand, different initial density, and also changing C/D. The results of these tests culminated in the chart shown below in figure 2-6. This paper concluded that increasing C/D had only a small effect on the required heading pressure.

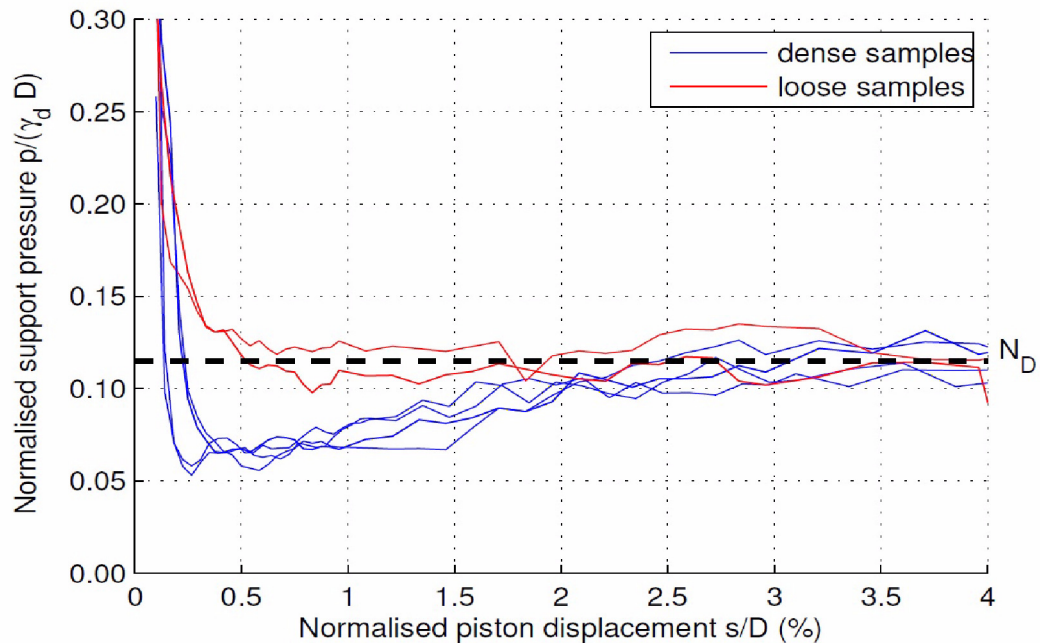


Figure 2-6. Results from Kirsch, 2010

Another issues of interest in tunneling research is the method of failure. Chen et al, 2013 created large scale 3D models with a tunnel diameter of one metre. A diagram of the models used are in figure 2-7.

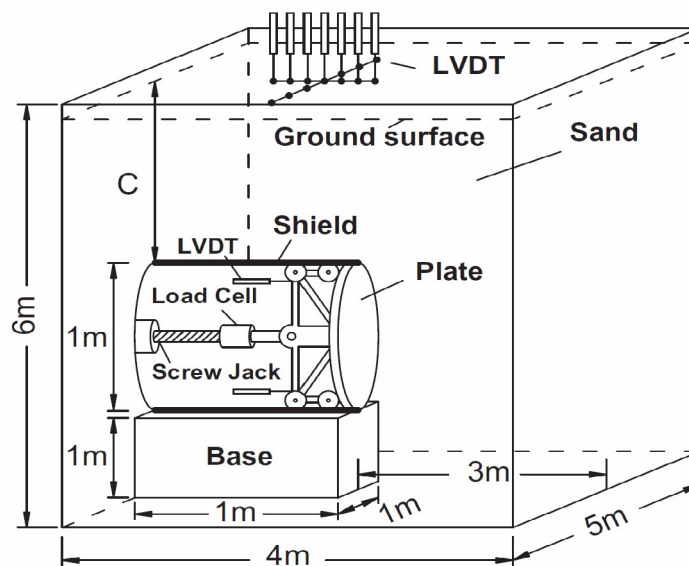


Figure 2-7. Diagram of physical model Chen et al, 2013

This paper investigated heading pressure and ground settlement over various C/D ratios 0.5, 1.0, and 2.0. The paper also compared their results with the results from Kirsh, 2010. This and the settlement results are in figure 2-8 below.

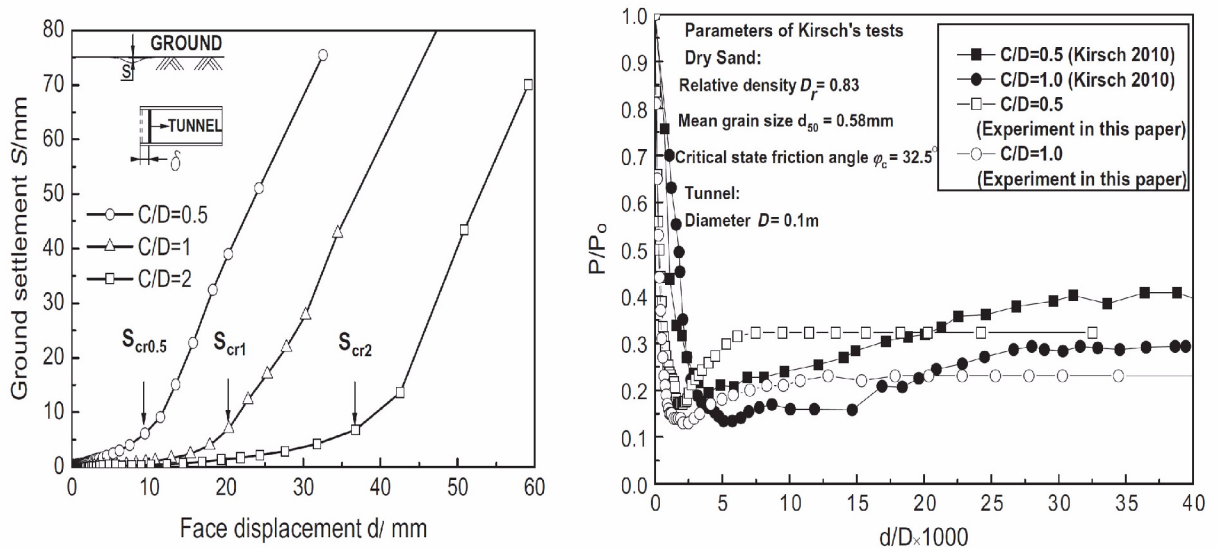


Figure 2-8. Heading pressure and settlement results from Chen et al, 2013

They also made some significant commentary on the effects of soil arching on this sort of testing. They placed 48 earth pressure sensors (LVDT's) in the soil at various depths in the $C/D=2$ case to measure soil pressure as the experiment was in progress to investigate the effects of arching. They described the failure process as a two stage process, where the two stages are local and global failure, which are dependant on the evolution of the soil arching.

The phenomenon of soil arching was described very well by Sadrekarimi and Abbasnejad, 2008: “When part of a soil mass yields, while other part adjoining the yielding part remains stationary, movement between yielding and stationary parts causes shear stress to develop. This shear stress opposes the relative movement of soil masses. Since the shearing resistance tends to keep the yielding mass in its original position, it reduces the pressure on the yielding part and increases it on the adjoining stationary part.” In other words, in granular soils a portion of the vertical stress on the soil is redistributed horizontally in an arch manner. This was shown well by Smid and Novosad, 1981 (cited in Michalowski, 2003), who conducted an experiment to measure the pressure under a conical pile of soil. His results indicate that there is some stress depression under the centre of pile. This is shown below in figure 2-9.

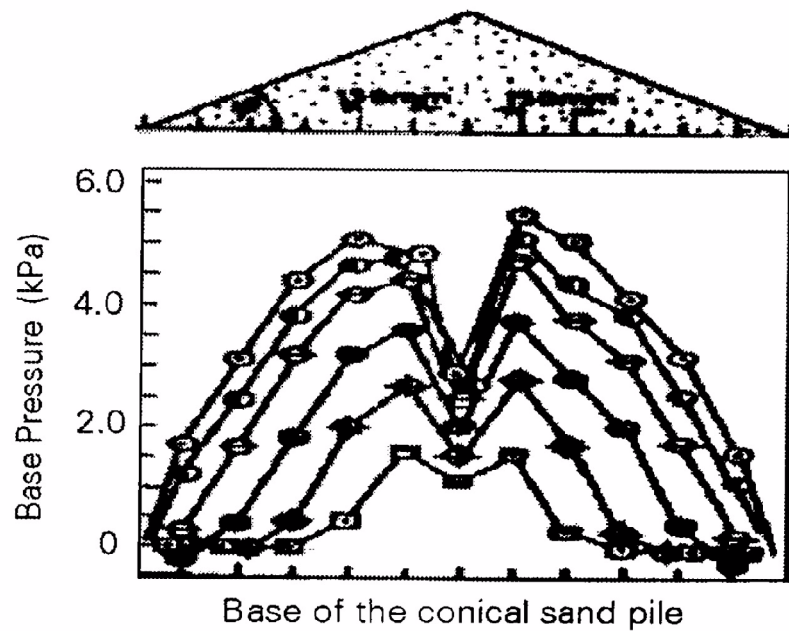


Figure 2-9. Pressure distribution under a pile of soil, Smid and Novosad, 1981

Another research paper of interest is one that used physical models with experimental transparent soil by Ahmed and Iskander, 2012. This soil resembled medium density sand, and was used to allow the use of digital image correlation, a technique similar to Particle Image Velocimetry. This research covered 4 C/D ratios from 1.5–4.5. The tunnel was simulated by a PVC tube with a latex membrane on the end to represent the tunnel heading. Heading pressure was induced by using a mineral oil. An image and a diagram of the model that were used are below in figure 2-10.

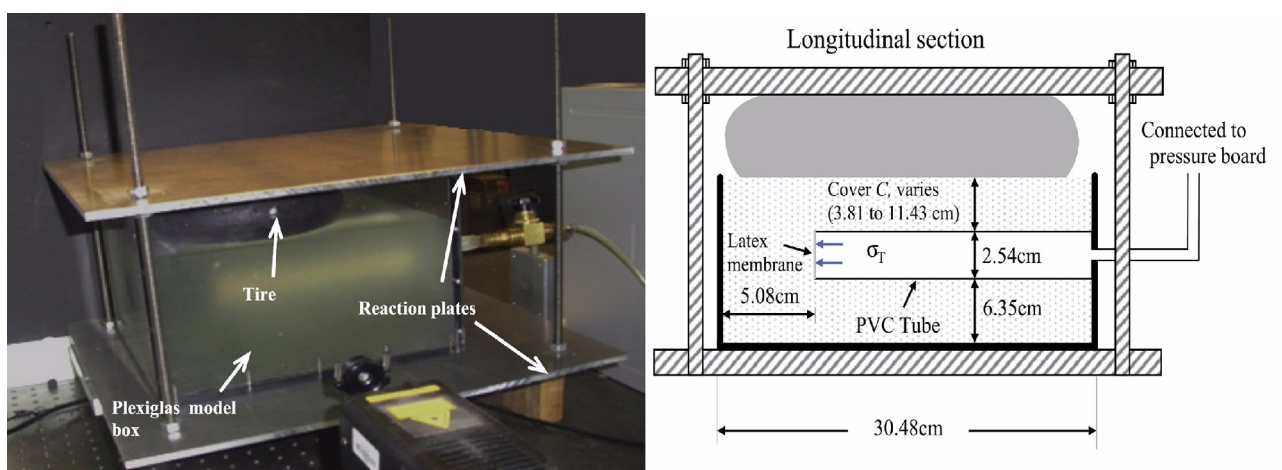


Figure 2-10. Model used in Ahmed and Iskander, 2012

The transparent soil was failed by using stress relaxation techniques, whereby the pressure applied to the tunnel heading is gradually reduced. Therefore, the results of interest are

heading pressure, and the corresponding displacement of the heading, in the different C/D cases. These are included below in figure 2-11.

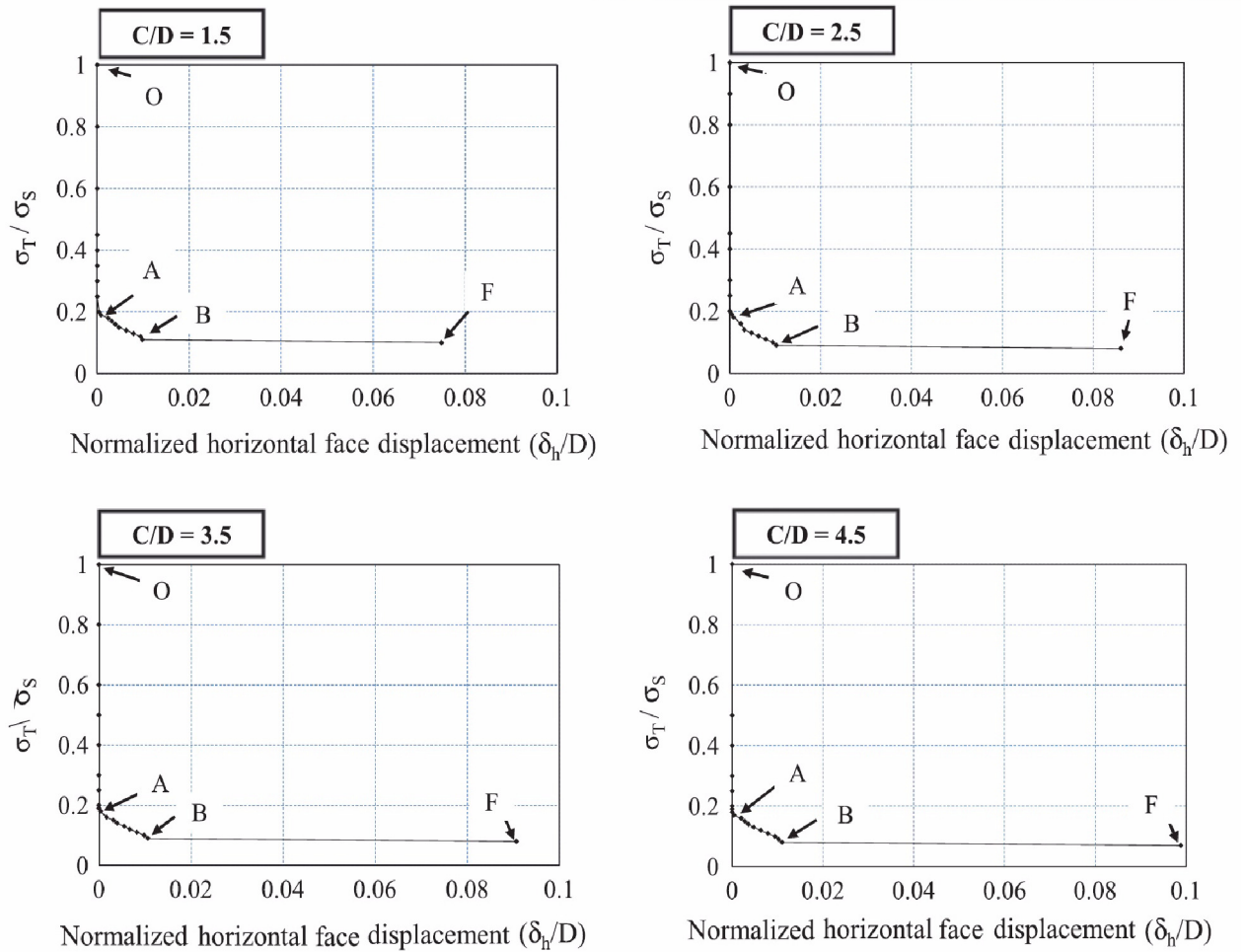


Figure 2-11. Heading pressure and displacement results from Ahmed and Iskander, 2012

From these results, the authors determined that the ground deformation could be divided into three stages: face deformation O to A where there is very little deformation, face slip A-B where there is increasing but stable deformation, and failure B-F where there is excessive and unstable deformation.

There are many more research papers that used physical modelling to investigate tunnel stability in sand including Chen et al, 2011; Messerli et al, 2010; Mollon et al, 2009; Takehiro, 2001; and Vardoulakas, 2009.

2.4 Particle Image Velocimetry

PIV is a powerful image processing technique that is used to visualise and measure two dimensional deformation. Particle Image Velocimetry (PIV) is not a new technique. PIV has its roots in fluid dynamics where it has been used for qualitative analysis of flow visualisation. Below in figure 2-12 is a simple example of PIV being used to determine the flow path of water in a creek.

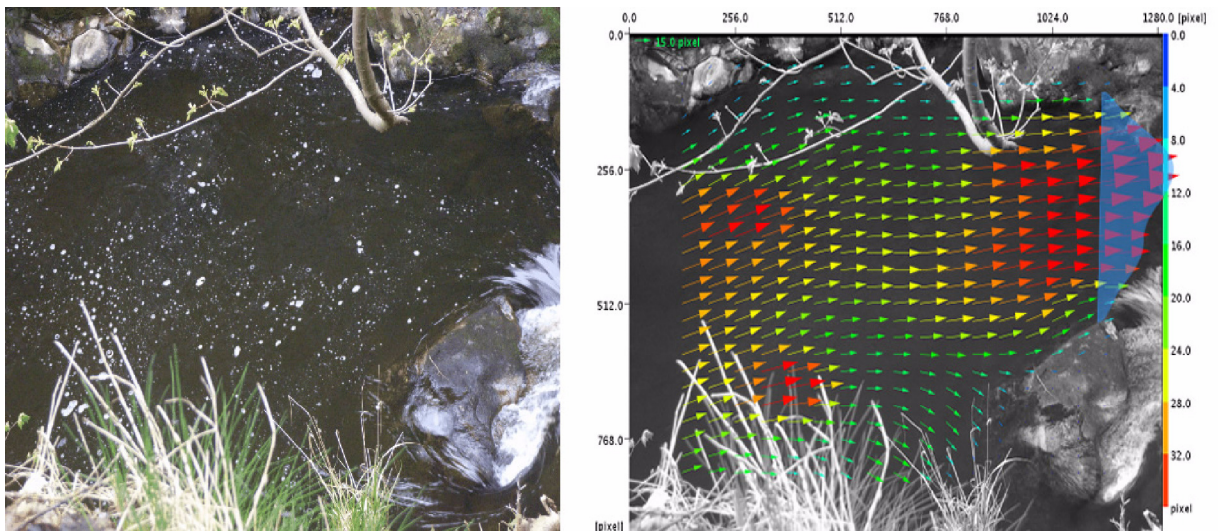


Figure 2-12. PIV being used to analyze flow path of a creek (jPIV, 2013)

The term Particle Image Velocimetry was suggested and adopted in 1984 replacing the use of the previous term “Laser Speckle Velocimetry” (Adraian, 2005). The PIV process determines the average motion of small groups of particles contained within small regions of a wider focus area. The quality of the tracking is dependent on the quality of the images and the concentration and size of particles. Fine particled soils such as clay will not work by themselves unless the image resolution is very high because the program cant easily distinguish the independant small regions from each other. Usually, techniques to circumvent such problems include ‘seed particles’, putting particles in the soil just for the programs benefit. This has been in several research papers. White, Randolph, and Thompson (2005) used a layer of plastic flock powder sieved onto the surface of the clay, and commented that using dyed sand would be just as effective.

PIV requires a minimum of two images of the same thing taken with a small time difference. The general process with all the programs is then to set your mesh, called the interrogation zone, and the individual regions called patches. The mesh gives starting coordinates for all the patches. The algorithm then determines the movement of the patch between the two images using statistical and cross correlation (Raffel et al. 1998) and/or photogrammetric transformation (White and Take, 2003) depending on the particular program.

There are a large number of programs available that do PIV analysis. Some of the programs that exist and that were considered in this research project were: MATPIV, OpenPIV, JPIV, PIVview, and geoPIV. The first three are all free to access and use, but are quite general purpose, and not as well suited to this project as some other alternatives. PIVview is proprietary software developed by PIVtech and only a demonstration version is freely available. The latter, geoPIV, was created by David White and Andy Take during the course of doctoral research. While it runs through MATLAB like some of the other alternatives it operates slightly differently to the other software, as it was created and written specifically for geotechnical research. It is available at no charge for educational purposes, and the authors provide a PDF manual for its operation. Because of these reasons, geoPIV was the software chosen for this project.

White and Take's 2003 paper 'Soil deformation measurement using particle image velocimetry' has been integral to the image processing component of this project. In it, the authors comment on the performance of previous image processing techniques such as X-ray and stereo-photogrammetric methods, with particular reference to accuracy, precision, and resolution. The first two are measured in terms of amount of error with respect to the field of view (FOV), where the smaller fraction of FOV error is better. Phillips (1991) determined that the measurement precision of X-ray techniques was 1/10,000th of an FOV. Butterfield et al. (1970) and Andrawes & Butterfield (1973) achieved a comparable precision of 1/11 000th of the FOV using stereo-photogrammetric methods. The experiments performed in this research used a 2 megapixel camera, which they concluded provided an accuracy of 1/17 600th of the FOV. The third component of performance was resolution, which is illustrated in figure 2-13. The number of measurement points that can be established in an image is a function of the PIV patch size. By using smaller PIV patches, the measurement array size can be increased, at a cost of reduced precision. Thus, compared with previous image-based methods of displacement measurement, this system offers an increase in performance in all aspects.

Some comments were also made regarding the size of the patches with regard to accuracy and precision. Seven tests were done with different conditions using different patch sizes.

The results are contained in figure 2-14. It can be seen that larger patch sizes results in a decrease in error. Consequently, however, this results in a decrease in accuracy as well.

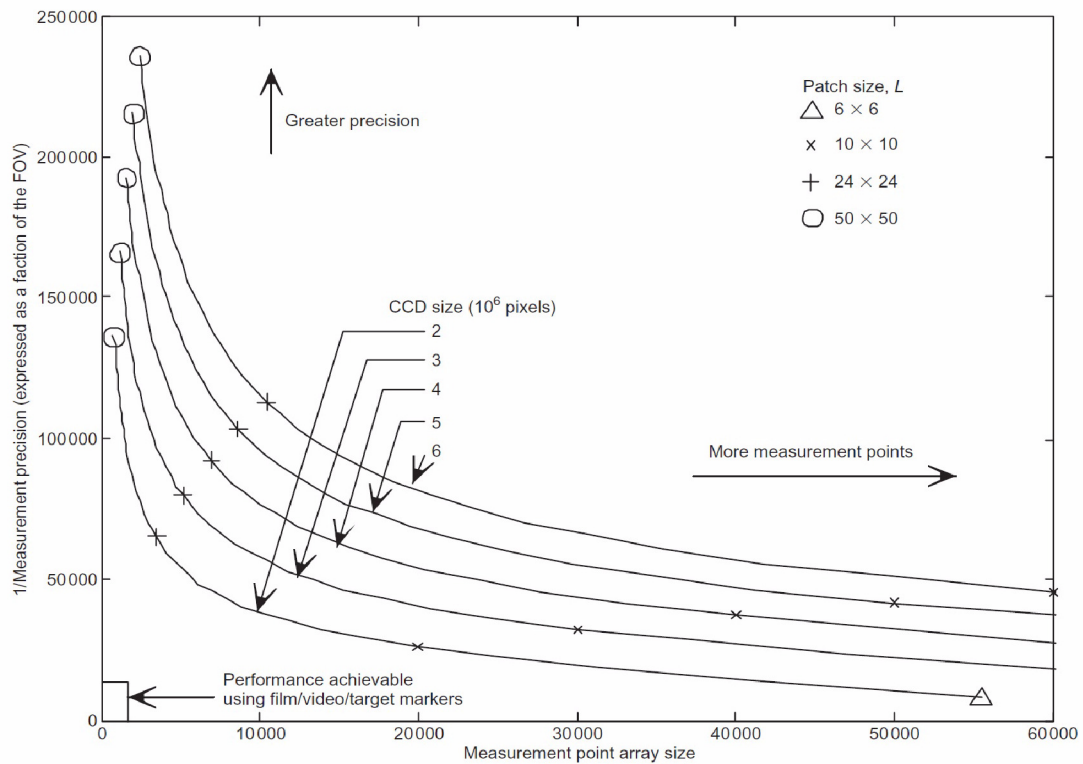


Figure 2-13. Resolution versus Precision (White and take, 2003)

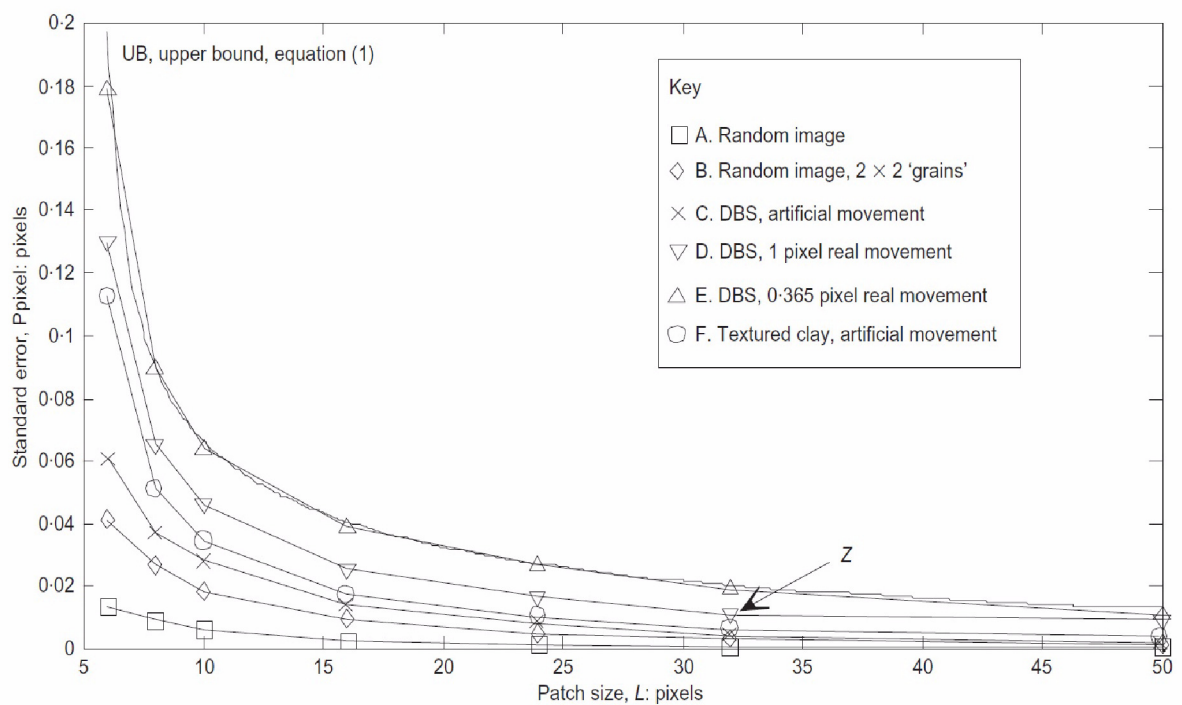


Figure 2-14. Patch size versus precision error (White and Take, 2003)

Several papers have used particle image velocimetry or similar techniques to quantitatively evaluate and analyze the soil failure in response to tunnel instability such as Ahmed and Iskander (2012), and Kirsch (2010). The primary output of a PIV analysis are vector fields, which are generally presented graphically in one and/or two forms: as vector plots (figure 2-15 left) or colour plots where the colour represents the magnitude of the soil movement (figure 2-15 right).

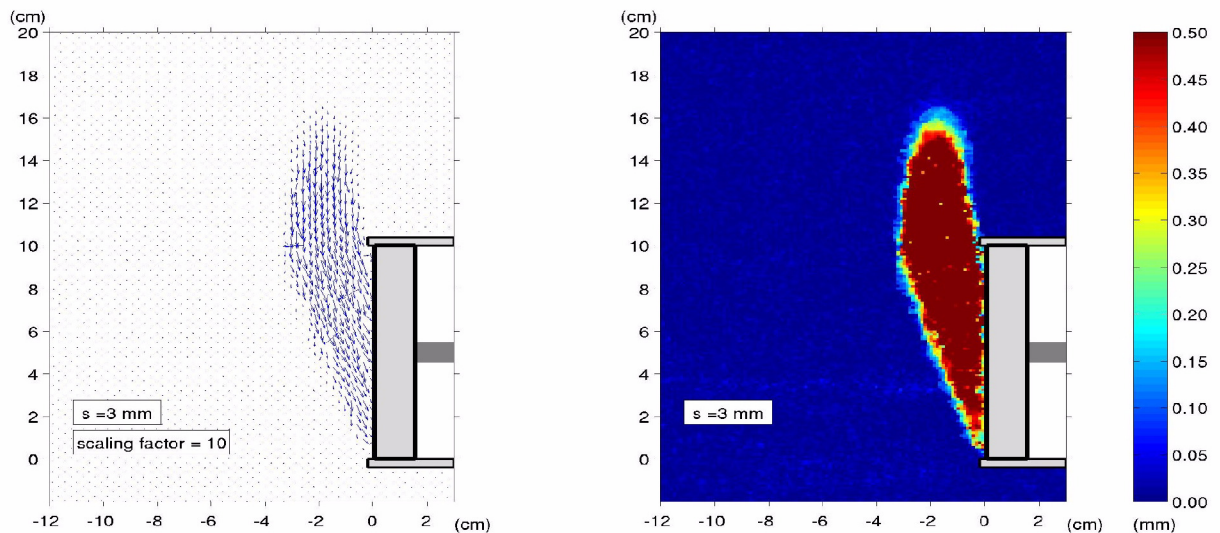


Figure 2-15. PIV results from Kirsch, 2010

2.5 Numerical Modelling

During most of the 20th century pretty much all research was physical or empirical. This was particularly true in the geotechnical area with some of the iconic geotechnical research regarding tunnels coming from that era: Peck (1969), Atkinson and Potts (1979), Leca and Dormieux (1990), and Chambon and Corte (1994). During the past 20 years this has changed dramatically with the rapid development of computing and information technology. Whilst physical modelling is still widely used in this field, computer and numerical analysis using the finite element method (FEM) and finite difference modelling have, to a degree, taken over the other empirical and mathematical modelling areas.

There are a relatively large number of software suites that employ these methods and that are commonly used in geotechnical research, with the most common being *ABAQUS*, *PLAXIS*, and *FLAC*. The former is a general purpose software, whilst the latter two have been specifically written for geotechnical applications. For this project, *FLAC* has been chosen, predominantly because of availability and expertise at USQ. *FLAC* is a two-dimensional explicit finite difference program for engineering mechanics computa-

tion. This program simulates the behavior of structures built of soil, rock or other materials that may undergo plastic flow when their yield limits are reached (Itasca, 2013). It is a very widely used software package, and has been in development since 1986. The program also contains its own programming language FLACish (FISH), which can be used to write and customize a modelling script.

In the paper by Kirsch (2010), ABAQUS was used to investigate heading stability of sand, and to compare the results with the physical modelling also in the paper. He also compared the results between the hypoplasticity and mohr-coulomb soil models, and found that it made little difference to the results. An image of the element model and the results/comparison are below in figure 2-16.

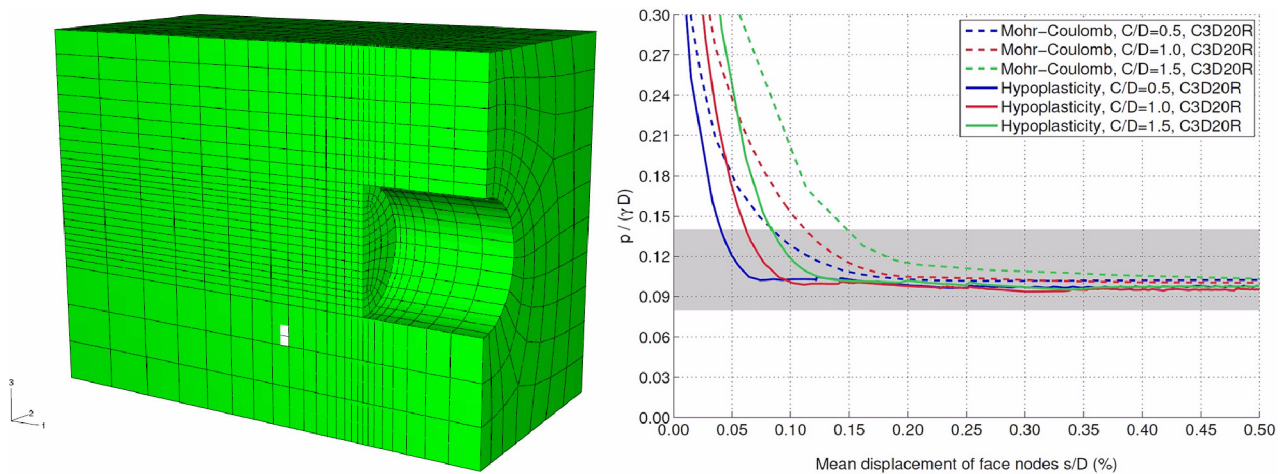


Figure 2-16. 3D model and results from Kirsh, 2010 using ABAQUS

Generally for the subject of tunneling, most researchers use either PLAXIS or FLAC. A paper by Wong et al (2012) used physical centrifuge modelling as well as PLAXIS to model the passive failure of a tunnel heading, that is when the applied heading pressure is too high. The heading pressure and diaplacment were monitored, and the subsequent surface displacements were measured. The mesh used and the results of the study are in figure 2-17. It can be seen that in the $C/D=4.3$ case, the computed heading pressure is substantially greater than the measured values. the authors believed that this may be due to some flaws with physical model whilst the centrifuge was stationary, namely some of the soil loosening and forming a weakspot around the tunnel face.

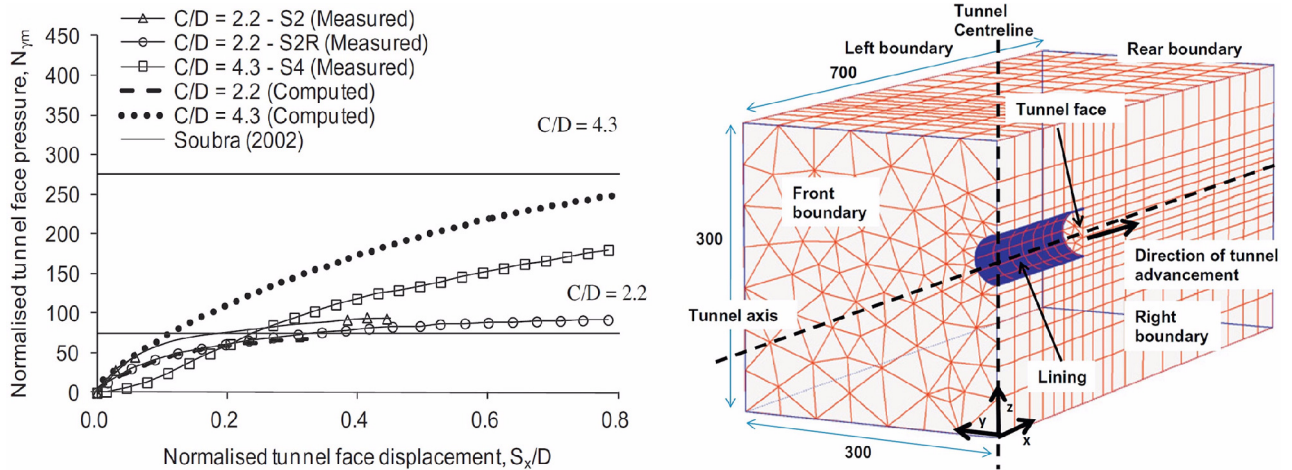


Figure 2-17. Results and mesh used from Wong et al, 2012

Ohta and Kiya (2001) is a notable paper that uses FLAC for their numerical modelling. The authors investigate, in particular, the effects of groundwater on stability. Figure 2-18 (right) illustrates the relationship between the strain at the face and the initial water levels for varying values of Young's modulus of the soil.

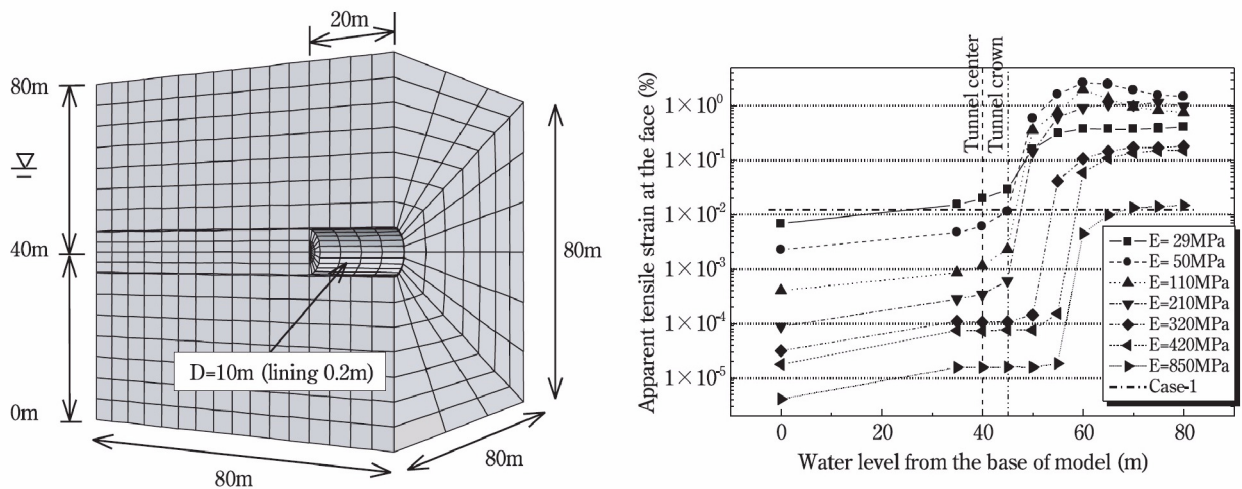


Figure 2-18. Mesh and results from FLAC analysis (Ohta and Kiya, 2001)

There are many more papers using numerical and computer modelling for their research. However one aspect that is always there is verification, either with physical modelling or with another author's research. Numerical modelling can be used to model scenarios that would be complex or expensive to model physically, but verification is always needed.

Physical Modelling



3.1 Introduction

Physical modelling has been used widely in geotechnical research for quite some time. Large scale tests are expensive, time consuming, and often don't deliver sufficient return, in terms of results, for the investment. The use of much smaller scale models is therefore much more common.

There are two main types of small scale tests: those that are run under standard gravity conditions, that is 1g, and those that use a centrifuge as shown in figure 3-1, under ng conditions. Tests conducted under 1g conditions are easily reproducible, have minimal preparations required, and are easily controllable. The drawback is that the stresses in the soil compared to the soil properties are not realistic, and hence they are subject to scaling laws. Centrifuge modelling can overcome some of these shortcomings. The small scale model can be subjected to higher gravity levels, ng . This then allows the self weight of the soil and the stresses within it to become comparable to a large scale model which is n times larger (Kirsch, 2009). However, the gravity level that each soil particle experiences is relative to its distance from the centre of the centrifuge, which means that there is a distribution of gravity acceleration through the model. This problem requires adjustment and calibration to the model dimensions and instrumentation to overcome it which is quite complex. Thus, centrifuge modelling is very expensive and time consuming.



Figure 3-1. Geotechnical centrifuge (Columbia University, 2005)

They are used themselves to study the behaviour of soil and its impacts, but quite commonly also to verify numerical models. If the soil of interest is sand, using 1g scale models is particularly attractive, as there is no need for a centrifuge as the soil fails under its own self weight, and the models can be relatively simple to construct and operate, whilst still yielding good results. Therefore in this project, 1g scale models have been used to conduct the physical modelling.

3.2 Setup and tested material

The aim of the experimental tests in this project was to gain an understanding of the failure mechanisms in front of the tunnel face, and to examine the settlement characteristics of the soil with varying overburden (C/D ratios). To do this, the modelling tanks needed to be designed and constructed and the properties of the sand in question needed to be identified.

3.2.1 Sandbox and Tunnel Model

The design of the models draws inspiration from other undergraduate projects at USQ as well as other postgraduate research projects, namely from Kirsch A, 2009/2010, and Chen et al, 2011/2013. A picture of the models used is below in figure 3-1.

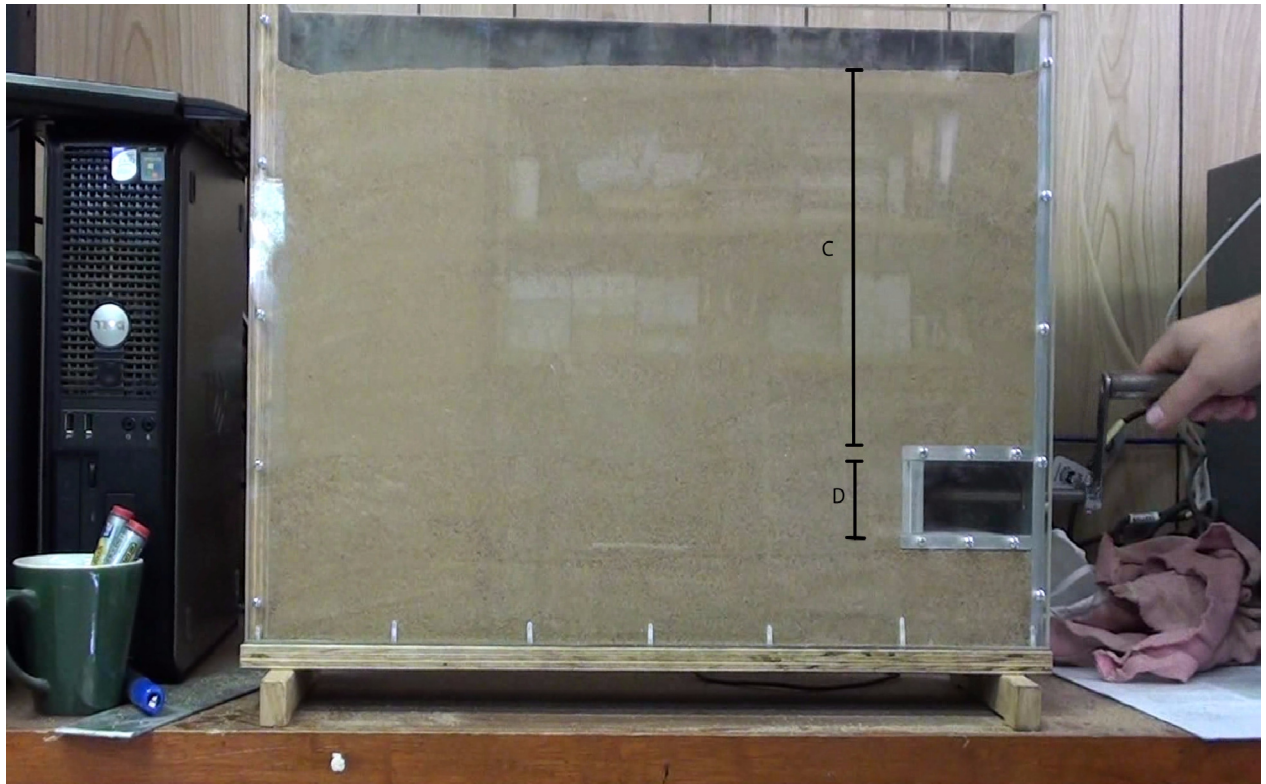


Figure 3-2. Soil sample and model tunnel at the start of the test

A total of three boxes were constructed to cater for the six C/D cases that were to be examined. They are 50 cm long and 5cm in breadth, with a totally transparent perspex front panel. Other dimensions of interest are contained in figure 3-2 below. The crank handle rotates the screw which slowly withdraws the heading. For this project, the tunnel has been approximated to a rectangle to simplify construction.

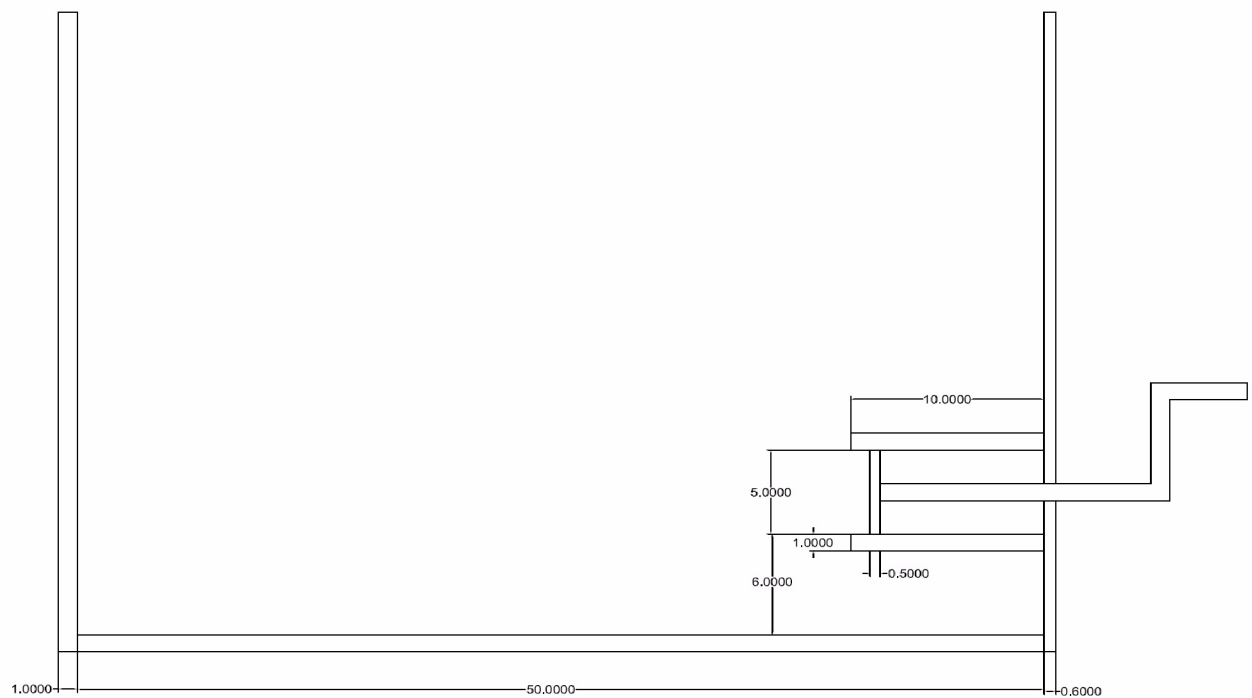


Figure 3-3. Front view of model

Future projects using similar apparatus would want a more sophisticated setup where the box was wider (3D), and the tunnel could be simulated using a cylinder of PVC. The capability to measure heading pressure with heading displacement would also be desirable, this would require a linear actuator with a load cell to replace the crank handle.

3.2.2 Sand Properties

As previously stated, the material of interest in this project is sand. For the sake of the numerical modelling, future results comparisons, and general completeness, the key properties of the sand have to be determined, with the key properties being friction angle and unit weight (density).

The sand used was USQ laboratory sand blended with coloured sand (for the PIV), and was constant for all experiments. The density was simply determined by carefully filling a container, avoiding any compaction, with known dimensions and self weight, measuring the total weight, and then calculating density. This was done five times using different sand each time and then taking an average. Results are below in table 3-1.

Table 3-1 |Results From density test

Sample no.	Density (kg/m ³)
1	1825
2	1780
3	1815
4	1806
5	1772
Average	1798.9

Therefore, a density of 1800 kg/m³ has been used for the numerical modelling. The friction angle was determined using a direct shear test. This is a very simple test that involves placing a small sample of soil in the apparatus, and then apply a shear load whilst a normal load is simultaneously applied. An image of the apparatus used, and a diagram of the core mechanism is below in figure 3-3.

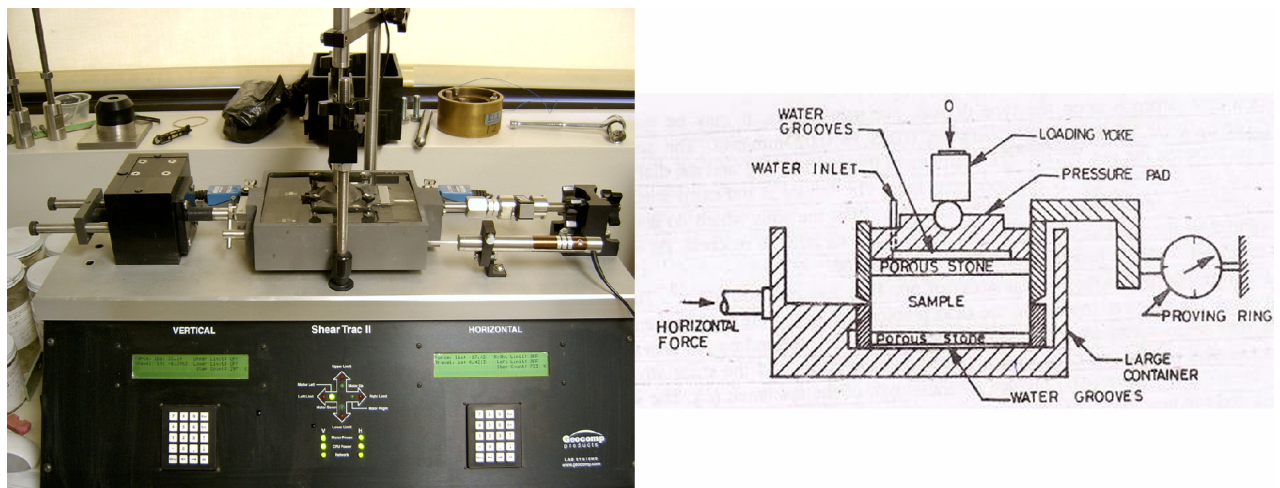


Figure 3-4. Apparatus used in a Direct shear test (left), diagram of the core mechanism (right)

The test is carried out multiple times while varying the applied vertical load. From this, the shear strengths of the soil with the varying vertical loads are known. This is shown in figure 3-4 below. The darker line represents the measured the shear strengths, while the grey line is a line of best fit. The angle that the line of best fit makes with the horizontal is the friction angle. Thus, it can be calculated that the friction angle is 35 degrees.

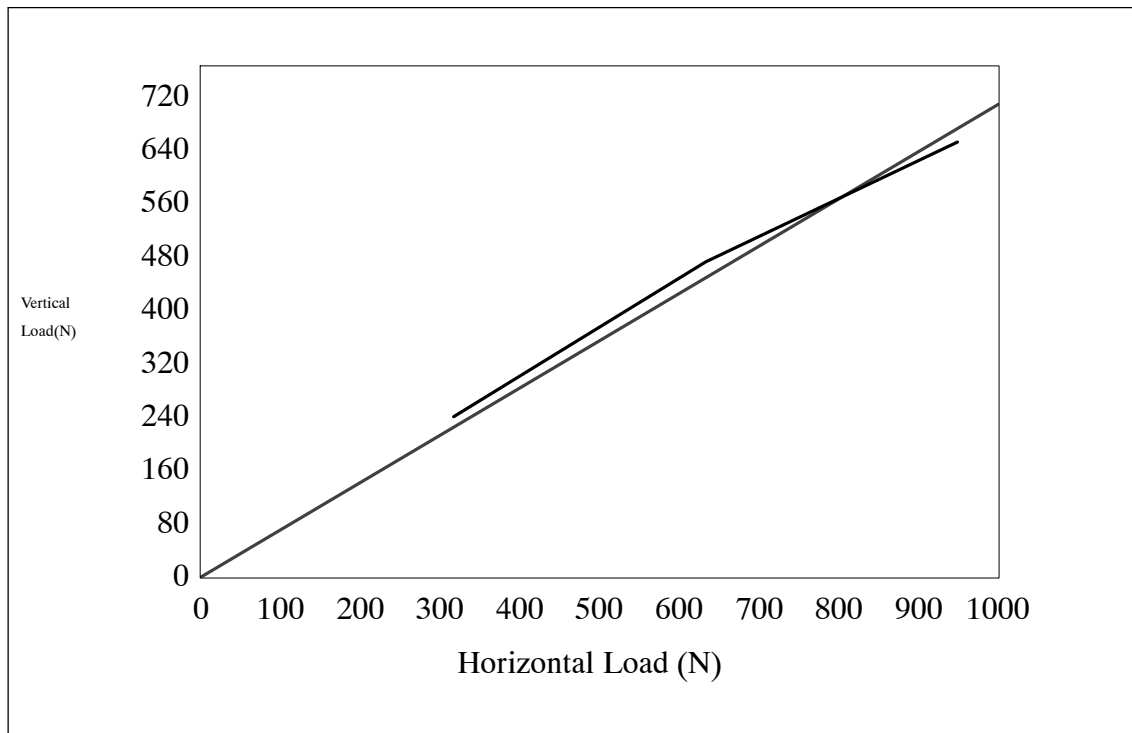


Figure 3-5. Results of shear box test on the sand

More tests could be conducted on the sand such as a sieve test to determine particle size distribution, but as this is a qualitative analysis of failure, this was considered unnecessary.

3.3 Test Procedure

The procedure for the physical modelling was kept as similar as possible through the six cases. Firstly, sand was poured as uniformly as possible into the model to the correct overburden level (100mm for $C/D=2$ etc) while avoiding any compacting or settling action. Then the heading is slowly withdrawn using the crank handle. The screw that has been used is calibrated for 1mm/revolution. Thus, the handle was rotated at approximately 1 revolution every two seconds, which therefore leads to the heading being retracted at 0.5mm/sec. This is stopped when the sand is no longer touching the heading, and this was considered as the total failure of the tunnel heading. After this, measurements were taken of settlement parameters.

While the heading is being retracted, a full HD camera is recording the soil movement from beginning to end. This footage is then used for the particle image velocimetry.

3.4 Results

After the tunnel heading has completely failed, i.e. there is no sand touching the heading, then the settlements are measured: S_{max} , B , and L as indicated in figure 3-6 below.

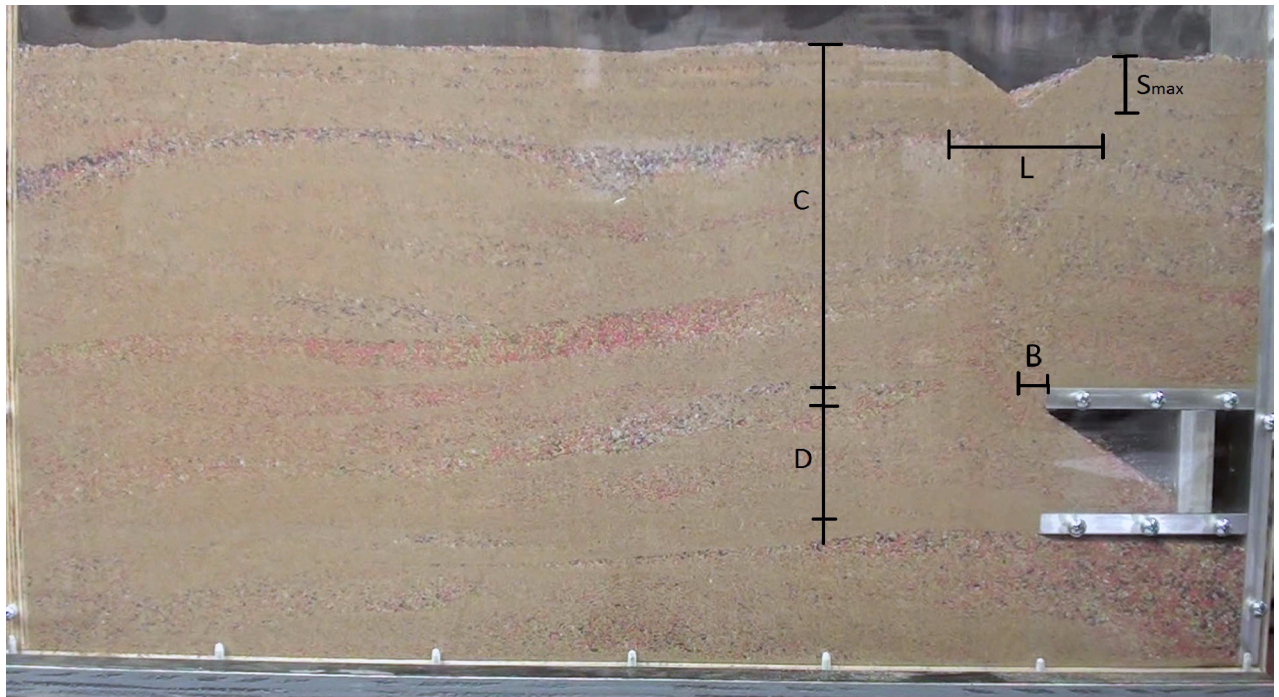


Figure 3-6. Measured settlement parameters

The results for these three settlement parameters are below in figures 3-7, 3-8, and 3-9 respectively. It can be seen that the maximum settlement, S_{max} , decreases with increasing C/D as the distribution of stress is spread over a wider area. The parameter B , representing distance of maximum settlement from initial tunnel face position, seems to increase and then plateau out with increasing C/D . This is due to soil arching effects becoming more dominant factor of the soil's movement. It's entirely possible with C/D of greater than 7, that the B parameter may in fact decrease. The L parameter indicative of the observable settlement zone seems to increase exponentially with C/D , which somewhat matches with the S_{max} results, the observed settlement “flattens out” with increasing C/D .

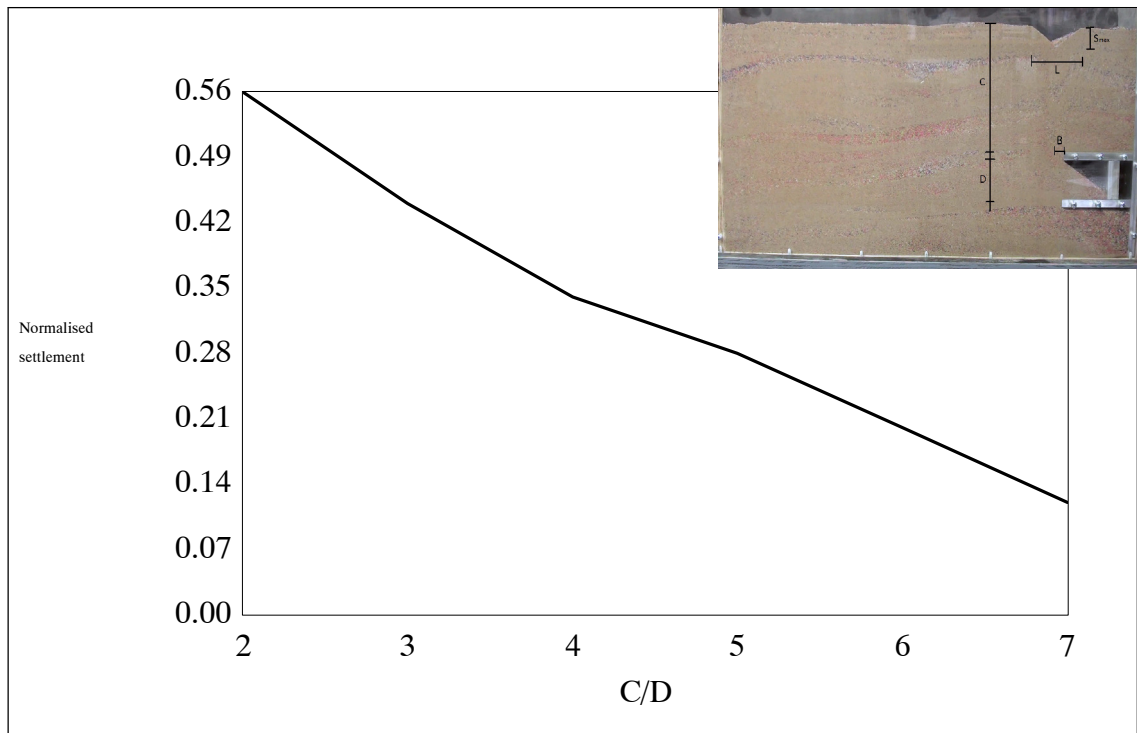


Figure 3-7. Results for Smax

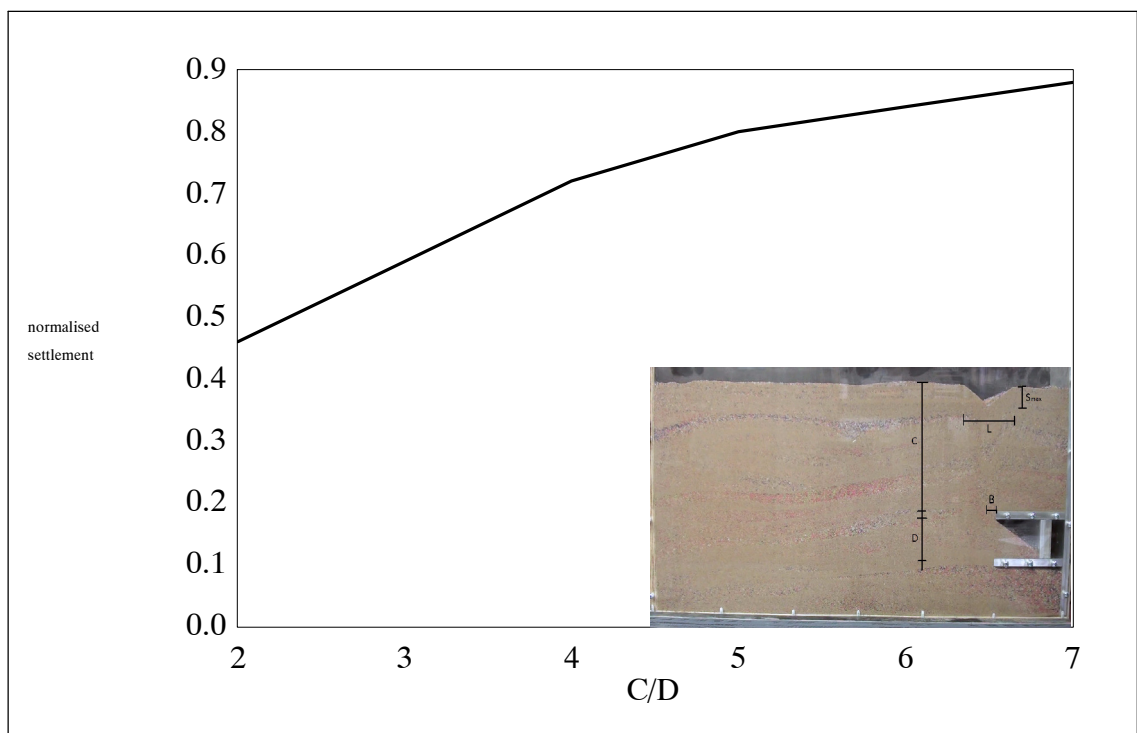


Figure 3-8. Results for B

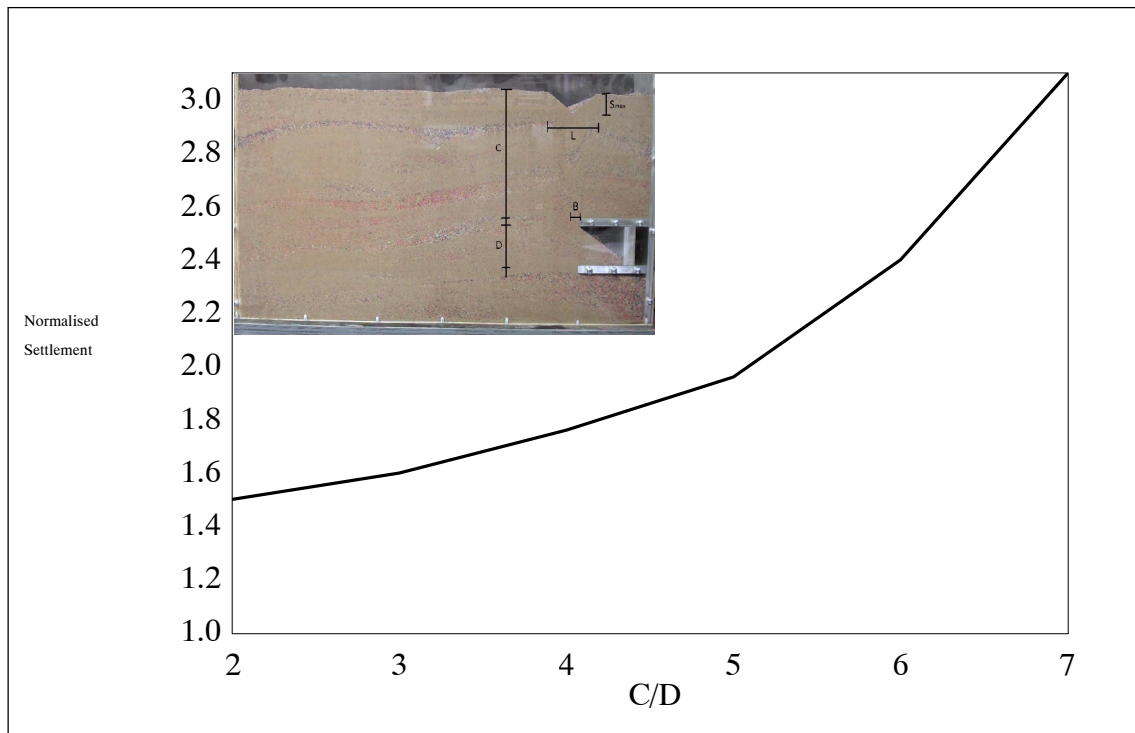


Figure 3-9. Results for L

3.5 Conclusions and Recommendations

Using some fairly basic scale models, some experimental tunnel failure modelling has been completed. Some settlement results over the six C/D cases have been collected and some comments and observations about their nature have been made. From here, the PIV can visualise the failure region, and can reveal some further observations about tunnel failure.

With the suggested upgrades to the models, some more significant results could be achieved, such as heading pressure against heading displacement for the six cases. This would open up more possibilities for comparison between the numerical and physical modelling.

Particle Image Velocimetry



4

4.1 Introduction

Particle Image Velocimetry is a technique that allows investigation of plane displacement patterns. (Kirsch, 2009). It was first used in fluid dynamics to demonstrate flow fields, but it has since become widely used in various fields, from aerospace, thermodynamics, and also geotechnical research. It is non-invasive, requires relatively minimal setup, and can analyze a soil sample on a grain-scale level (Nubel, 2002 (cited in Kirsch, 2009)). This combined with rapid technological advances in computing during the last 15–20 years, has meant that PIV has become very widely used in the geotechnical area.

There are many possible software alternatives that can do PIV analysis, but the program that was selected was geoPIV, created by David White and Andy Take. There were many reasons for this; because the methods it uses means that its performance is better compared to some others, relative ease of use and access as the authors provide the software and manuals free of charge for educational purposes.

In this research project, a qualitative investigation using PIV of the tunnel face collapse is used to identify displacement patterns and demonstrate failure behaviour. Layers of coloured sand could have been used, and has been, in the past for this purpose, but PIV is easier and less time consuming to setup, can demonstrate movement of the entire soil sample rather than just layers, and is more precise.

4.2 Equipment and Setup

An essential component of a particle image velocimetry analysis, is reporting the setup and equipment used. It will mean that others can compare the quality of results based on your equipment used, for example the resolution of the camera used etc.. For this project, the footage is obtained as the tunnel heading is being failed, where the camera is in position recording the process.

A full HD, 1920x1080 resolution 50fps, *Sony* video camera was used to record the process. The camera was kept approximately one metre from the face of the model as shown in figure 4-1.

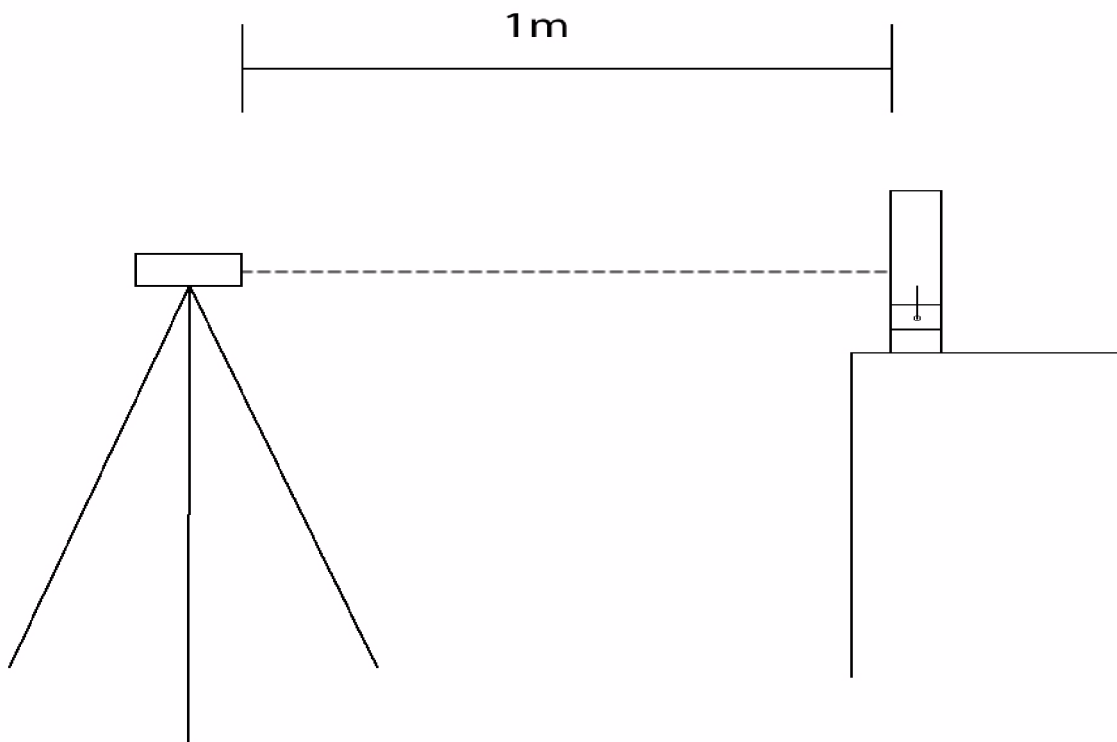


Figure 4-1. Setup of camera

During the first operations of the software, it became clear that it was very sensitive to the lighting conditions. Therefore, careful positioning of the model and camera was needed to ensure that we had minimal reflections on the transparent panel but also ample light so that the footage is clear. There was also the issue of the operating personell moving, and creating shadows as well, this had to be managed such that the model was somewhere where the personell could operate the crank handle but not negatively impact the lighting on the model. Figure 4-2 still shows some reflections, but the objects causing them are stationary and unlikely to cause issue. Another problem was the vibrations caused by the operating of the crank and the inherent resistance in the system. This problem proved somewhat

difficult to fully eradicate, but was minimised by having stabilisers on the bottom of the model (in picture), placing the model on a fixed bench, and using the relatively slow handle rotating speed.



Figure 4-2. Zone of interest in the PIV analysis

To do the PIV analysis, images are extracted out of the video footage. Because of the low resolution of the camera and therefore the images, only 2 Megapixels, and the fine grained nature of sand, it was discovered that the camera needed to be focussed on the failure chimney region, i.e. the red coloured region in figure 4-2. The main problems that were caused prior to this were wild vectors in the vector fields of the PIV analysis. This is shown in figure 4-3 below.



Figure 4-3. Wild Vectors in the PIV analysis

This particular problem in this case is primarily caused by a low spatial variation in brightness across the image. In other words, the program has difficulty differentiating patches, and consequently incorrectly interprets their movement.

4.2.1 Recommendations for future use

Using a higher resolution camera would provide significant and numerous benefits. Firstly, larger patch sizes (in pixels) could cover the same region of the model, which would result in an increase in precision for no loss in accuracy. For example, with a 1920x1080 camera, a 40 pixel square roughly covers a 1.7x1.7 cm square in figure 4-3. If we had a camera with four times the resolution (3840x2160 pixels), a 40x40 pixel square covers one quarter of the area (0.85x0.85 cm), and hence an 80x80 pixel square would cover the same physical area (1.7x1.7 cm). As discussed in the general review, an increase in the patch size (the individual unit in the mesh/interrogation zone) results in an increase in precision, but the patch concentration hasn't reduced, hence no loss in accuracy.

This camera would need to be setup such that it automatically captured an image at every specific time step, every one second for example. Getting some proper lighting equipment to eliminate shadows and reflections would be highly beneficial as well.

The geoPIV software package has the functionality to give strain rate contours, but it requires some calibration, which wasn't deemed necessary as only a qualitative analysis was needed. However, future research requiring a quantitative analysis would need to do this.

4.3 Procedure of Analysis

As the analysis software requires images rather than a video file, the first step once the testing is completed is to export images out of the video. A freeware program named "VirtualDub" has been used for this purpose. As the raw footage has been recorded at 50 frames per second (fps), only every 100th frame is exported, this corresponds to one image every two seconds. More frames may increase accuracy but there will be diminishing returns the more frames that are included, and this will also dramatically increase the computing time. Then *Adobe Photoshop* was used for a slight adjustment to the levels to increase spatial variation in brightness and contrast across the image.

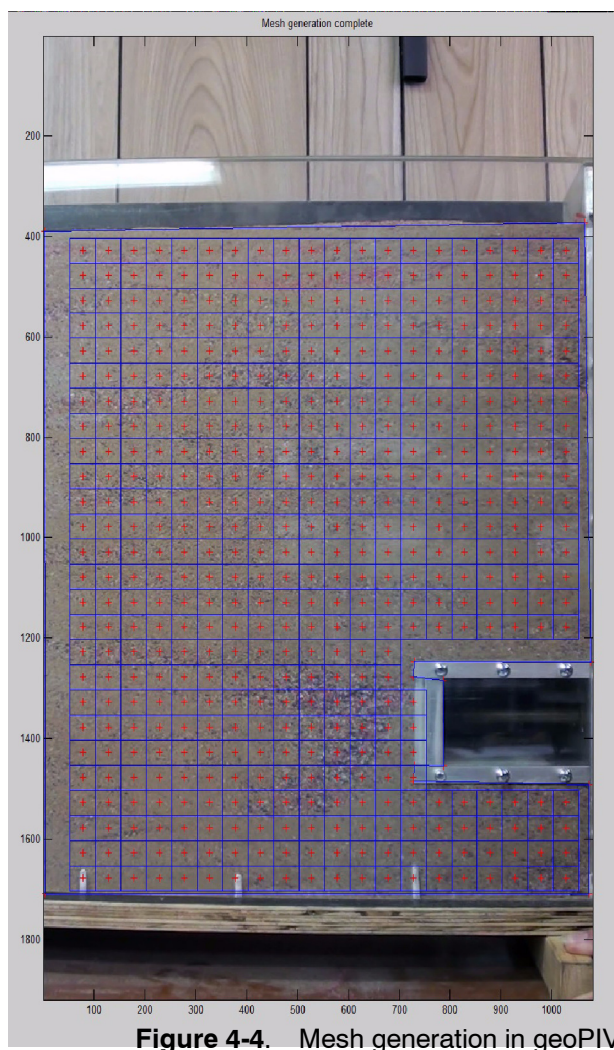
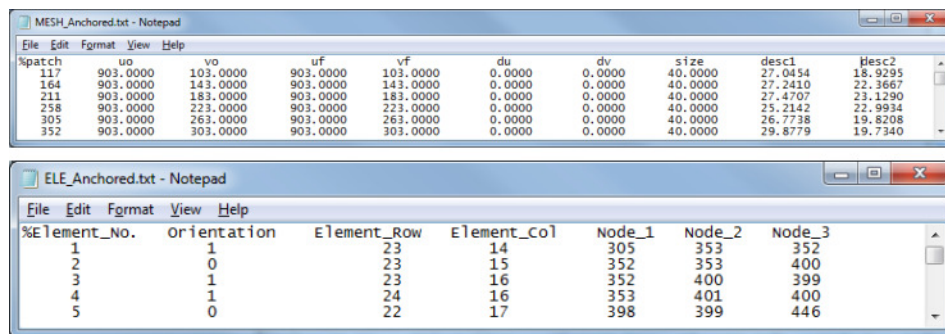


Figure 4-4. Mesh generation in geoPIV

After that, the images are ready to be processed using the software. The first stage is to run the mesh generation command, which requires you to select the size of the patches. An example mesh is shown above in figure 4-4. A patch size that is too large results in poor resolution, as the movement of the whole patch is aggregated into one vector, this may not be representative of all of the soil in the patch. On the other hand, patch sizes that are small are much more sensitive to lighting changes and other distortions; it also results in decrease in precision. The resultant problem that indicates a bad patch size is wild vectors, that is vectors that are incorrect. Choosing a patch size is about optimizing precision and resolution, whilst getting no wild vectors. For the purposes of this project, a patch size of 50x50 pixels has been used.

The resultant files from the mesh generation command are the mesh and element files, examples of which are shown below in figure 4-5.



MESH_Anchored.txt - Notepad

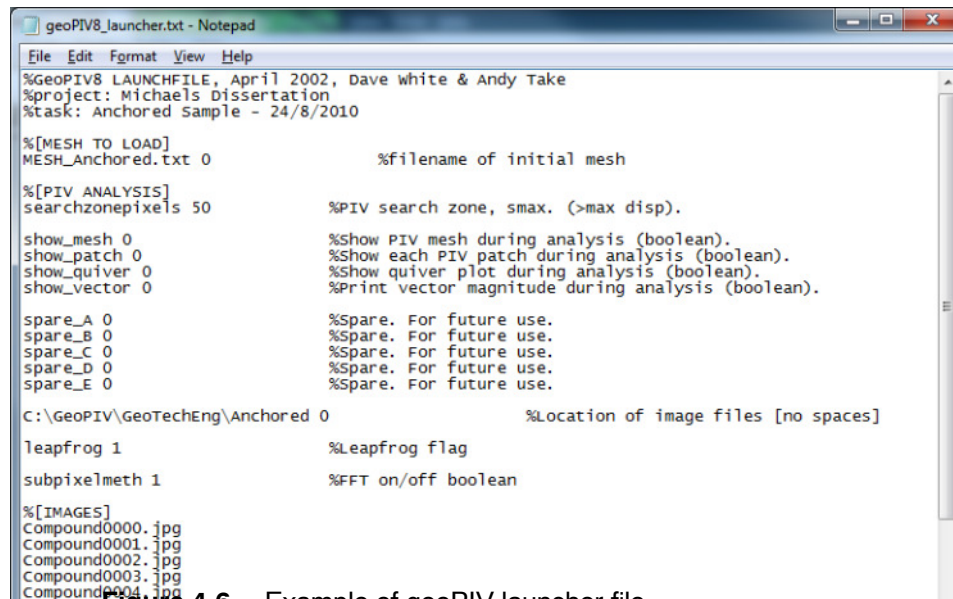
%patch	uo	vo	uf	vf	du	dv	size	desc1	desc2
117	903.0000	103.0000	903.0000	103.0000	0.0000	0.0000	40.0000	27.0454	18.9295
164	903.0000	143.0000	903.0000	143.0000	0.0000	0.0000	40.0000	27.2410	22.3667
211	903.0000	183.0000	903.0000	183.0000	0.0000	0.0000	40.0000	27.4707	23.1290
258	903.0000	223.0000	903.0000	223.0000	0.0000	0.0000	40.0000	25.2142	22.9934
305	903.0000	263.0000	903.0000	263.0000	0.0000	0.0000	40.0000	26.7738	19.8208
352	903.0000	303.0000	903.0000	303.0000	0.0000	0.0000	40.0000	29.8779	19.7340

ELE_Anchored.txt - Notepad

%Element_No.	orientation	Element_Row	Element_Col	Node_1	Node_2	Node_3
1	1	23	14	305	353	352
2	0	23	15	352	353	400
3	1	23	16	352	400	399
4	1	24	16	353	401	400
5	0	22	17	398	399	446

Figure 4-5. Examples of mesh and element files created by geoPIV

After the mesh is generated, and the MESH and ELE files have been created, the launcher file can be configured. A sample launcher file is below in figure 4-6. The filename of the mesh file and all the images to be processed must be listed. However, the two parameters of particular interest are “searchzonepixels”, and “leapfrog”. The former is the distance in pixels that the program will look for the displaced patch. Therefore, it should be set higher than the largest expected displacement. In this project, the images are only a relatively short amount of time apart (2 seconds), and therefore this parameter is largely negated. However, it has simply been set to 50 pixels, and this seems to have worked quite well. The other term of interest is “leapfrog”. This number indicates how often an image is updated. For example: if it is one, then the current image is simply compared to the following one and so on. Having it set to one can cause a decrease in precision if the number of images is very high (>100) as the error is accumulated through each image processing step. Setting it too high can result in wild vectors as the program can have trouble locating the patch several images on. In this project, it has simply been set to one. There are usually around 30-45 images for each case which is relatively few, and the patch size being used is relatively large, which will negate any precision losses.



```

geoPIV8_launcher.txt - Notepad
File Edit Format View Help
%GeoPIV8 LAUNCHFILE, April 2002, Dave white & Andy Take
%project: Michaels Dissertation
%task: Anchored Sample - 24/8/2010

%[MESH TO LOAD]
MESH_Anchored.txt 0          %filename of initial mesh

%[PIV ANALYSIS]
searchzonepixels 50          %PIV search zone, smax. (>max disp).

show_mesh 0                  %Show PIV mesh during analysis (boolean).
show_patch 0                 %Show each PIV patch during analysis (boolean).
show_quiver 0                %Show quiver plot during analysis (boolean).
show_vector 0                %Print vector magnitude during analysis (boolean).

spare_A 0                    %Spare. For future use.
spare_B 0                    %Spare. For future use.
spare_C 0                    %Spare. For future use.
spare_D 0                    %Spare. For future use.
spare_E 0                    %Spare. For future use.

C:\GeoPIV\GeoTechEng\Anchored 0 %Location of image files [no spaces]

leapfrog 1                   %Leapfrog flag

subpixelmeth 1               %FFT on/off boolean

%[IMAGES]
Compound0000.jpg
Compound0001.jpg
Compound0002.jpg
Compound0003.jpg
Compound0004.jpg

```

Figure 4-6. Example of geoPIV launcher file

Once the launcher file has been configured it can be executed. The outputs are text files for each image which contain the displacement information for each patch. Displaying the results can be done with some basic commands in the program set. However, they are basic, and to get anything other than that, a custom MATLAB script needs to be written, which has been done, and this is contained in the appendix.

4.4 Results

Using the display script contained in the appendix, the following vector plots can be obtained. Figure 4-7 contains the cases of C/D of 2 and 3 while figure 4-8 has the C/D of 4-7.

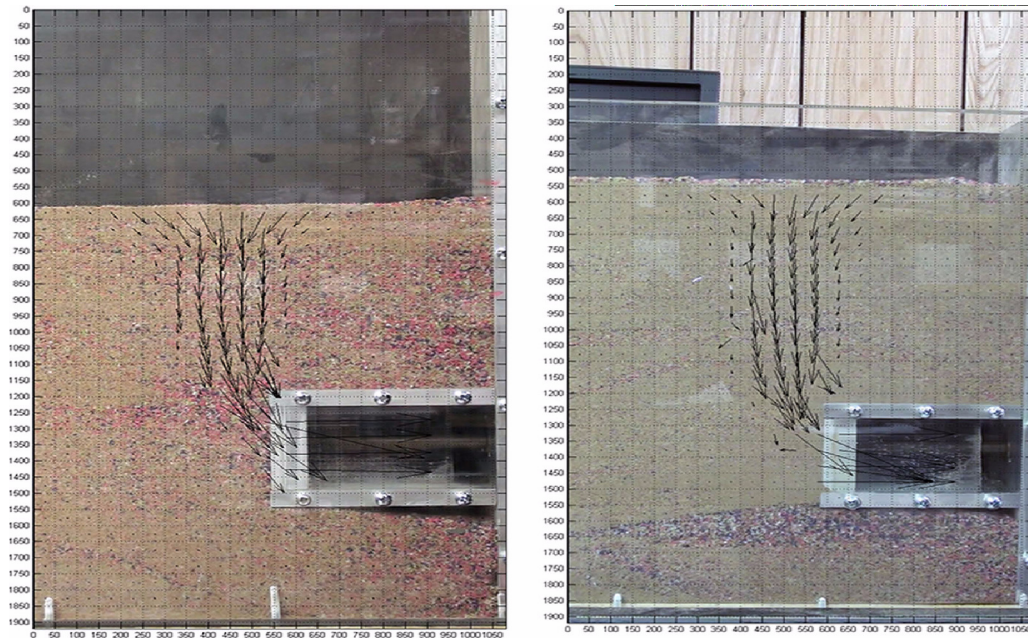


Figure 4-7. PIV vector plots for C/D 2-3 (left to right)

From the physical modelling results, we measured that maximum settlement decreases with increasing C/D , the position of this maximum settlement from the initial tunnel face increases but seems to plateau out at higher values of C/D , and the observable length of the settlement appeared to increase exponentially with C/D . These PIV plots of the physical modelling appear to somewhat confirm those observations.

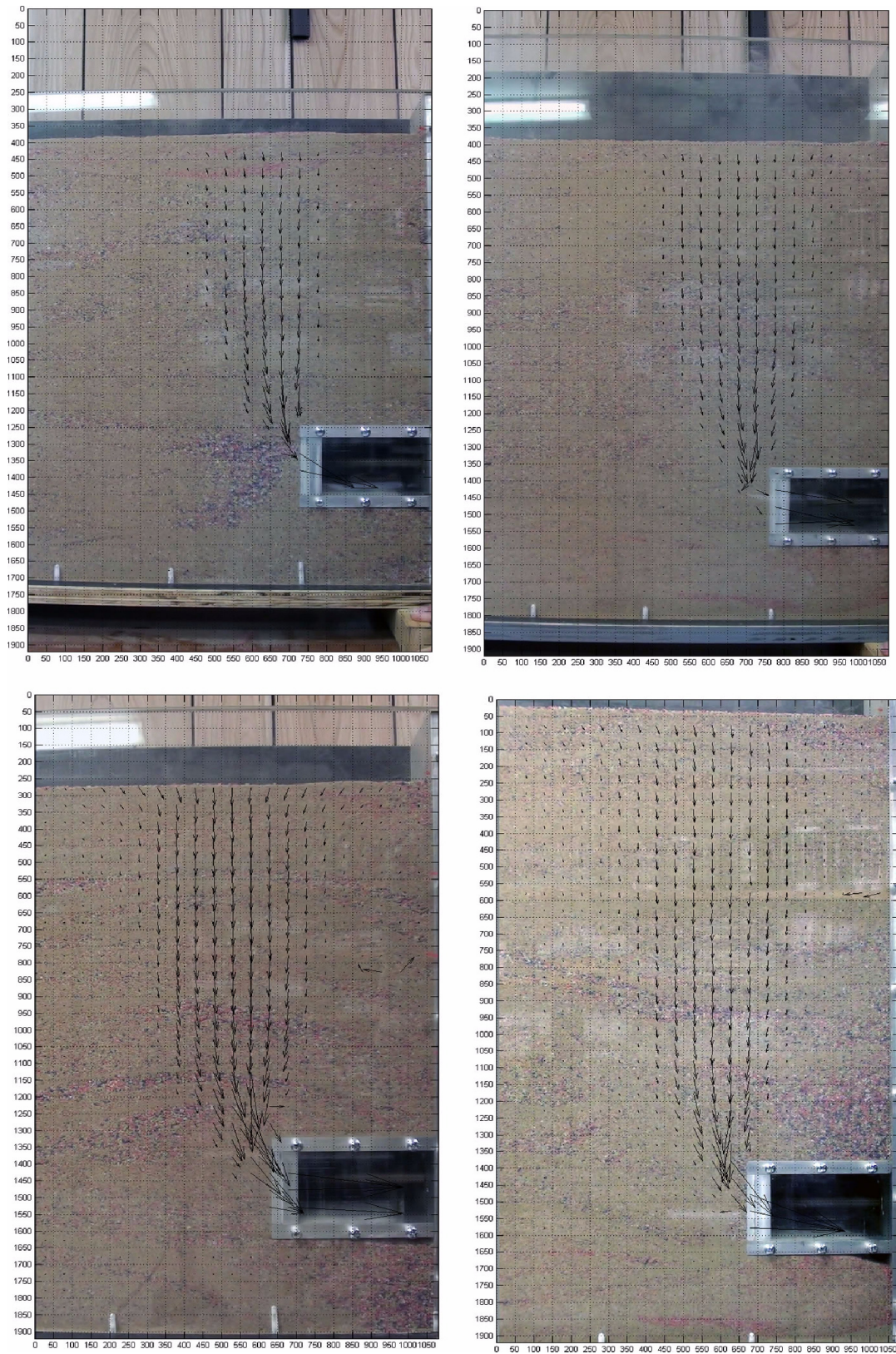


Figure 4-8. PIV vector plots for C/D 4-7 (left to right)

4.4.1 Failure behaviour

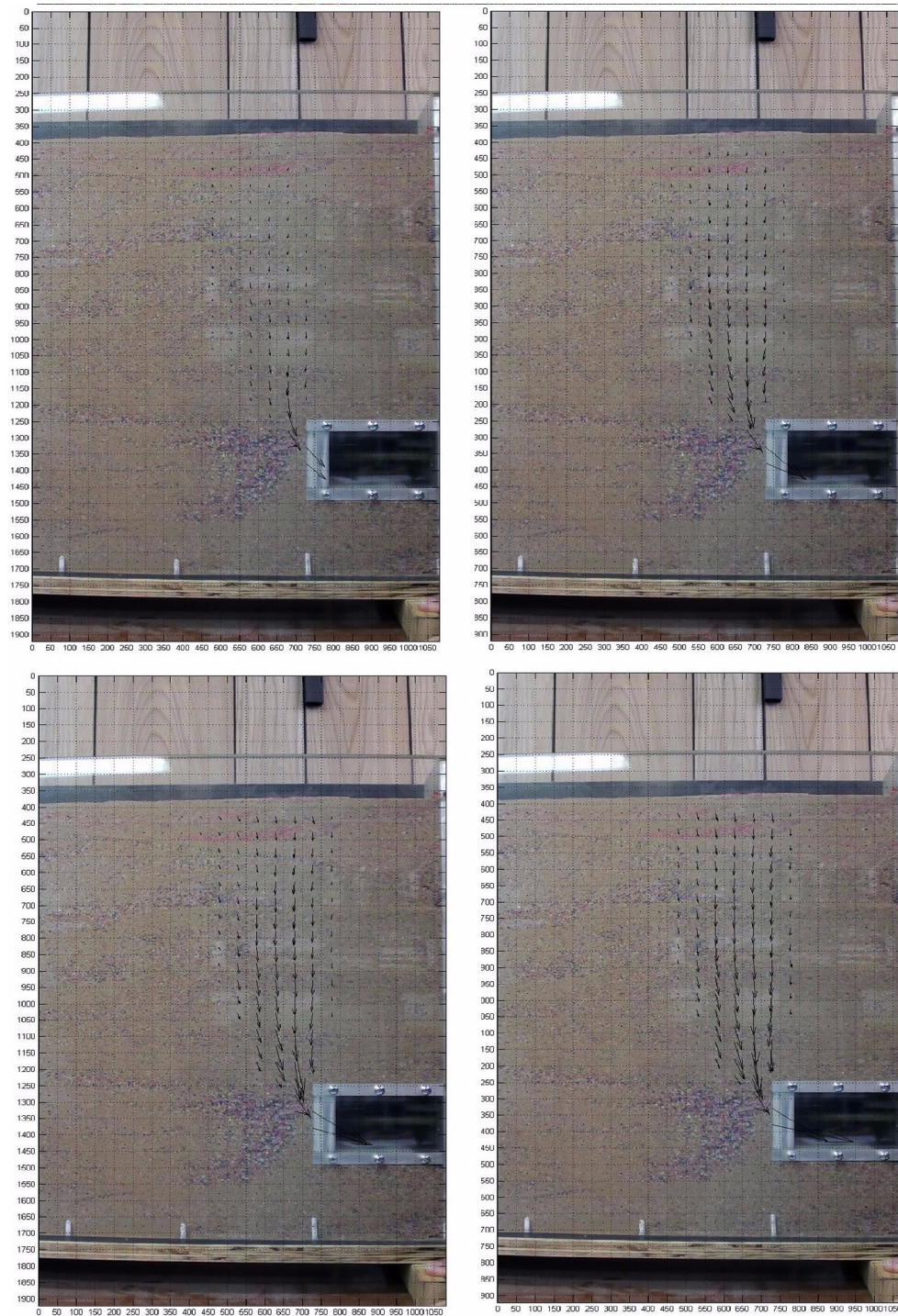


Figure 4-9. $C/D=5$ case, with PIV plots for 1/4, 1/2, 3/4 and full heading retraction time

Figure 4-9 above shows the $C/D=5$ case with four plots that represent the vector plots after one quarter of the images. This analysis used 36 images, so the first image is the plot after 9 images have been processed, then 18, 27, and finally the full 36. So it shows the progressive failure of the heading and movement of the soil. At one quarter time, there is

basically only local failure. The half time image shows the failure chimney beginning to form, but the impact at the surface is still only minimal. Three quarter time, and the chimney is now wider and the vectors now extend to the surface, the vectors at the tunnel heading are extensive. The full failure shows the fully developed failure chimney, and the settlement at the surface is now dramatic.

4.5 Conclusions and Recommendations

Particle Image Velocimetry has been shown to be employed quite effectively to demonstrate the plane movement of the soil in the models. A description of the setup, the problems faced, and the subsequent changes are given, and some suggestions for improvements are made. The procedure for the operation of geoPIV has been described with some of the key parameters highlighted. The results allow a comparison to the physical modelling measurements taken, and the conclusion is that they seem to generally agree. The failure behaviour can also be observed using PIV, and it can be noted that the failure pattern is a local failure around the tunnel face first and then the subsequent global collapse which concurs with comments made in the paper by Chen et al, 2013.

Improvements that can be made include using a higher resolution camera with an automatic fps controlled capturing mode which would allow higher precision and resolution in geoPIV. Having proper lighting would also allow better control of reflections and shadows. Setting up the equipment such that geoPIV could be calibrated would allow the use of the strain rate contours feature, which would open up further possibility for comparison with the numerical modelling.

Numerical Modelling



5

5.1 Introduction

For the majority of the 20th century, pretty much all engineering research was either physical or empirical. This was particularly true in the geotechnical area. However, during the last 20 years, significant development of computers has changed this dramatically, with numerical modelling using finite element and finite difference methods somewhat taking over from the empirical and areas. For geotechnical purposes, the three software that have become the popular and most well funded are: *ABAQUS*, *PLAXIS*, and *FLAC*.

This project will use *FLAC* as a comparison for the PIV and physical modelling results. In particular, it would be desirable to know if the *FLAC* program represents what was seen and measured in the physical modelling. Verifying the model with more results is good, as using a computer program is cheaper, easier, and more time efficient than physical experimentation, and it can then be adapted to more complex scenarios.

FLAC is a two-dimensional explicit finite difference program for engineering mechanise computation. This program simulates the behaviour of structures built of soil, rock, or other materials that may undergo plastic flow when their yield limits are reached (Itasca website, 2013). In essence, *FLAC* is a software package that can simulate the bahaviour of soils and geotechnical structures accurately.

There are a number of packages that can do this for very specific circumstances eg slope stability, but they are limited in scope. *FLAC* is quite powerful as it is very general, wide in scope, and has nearly unlimited customization. The downside of this, is that it has somewhat of a steep learning curve for beginning users. For this reason, the program used to model the tunnel failure has already been developed by Dr Jim Shiau, and I will input parameters as discussed in section 5.2.

5.2 Model Setup

This section will contain a brief outline of the problem, and then there will be a description of the setup used and discussion on the relevant parameters that were used in the numerical model.

5.2.1 Statement of problem

The problem to be modelled is tunnel instability. As previously mentioned, this involves the heading pressure that is applied to the tunnel face. In *FLAC*, this is modelled using stress relaxation techniques, whereby the heading pressure is gradually reduced by a percentage each step. An ideal sketch of the problem below in figure 5-1.

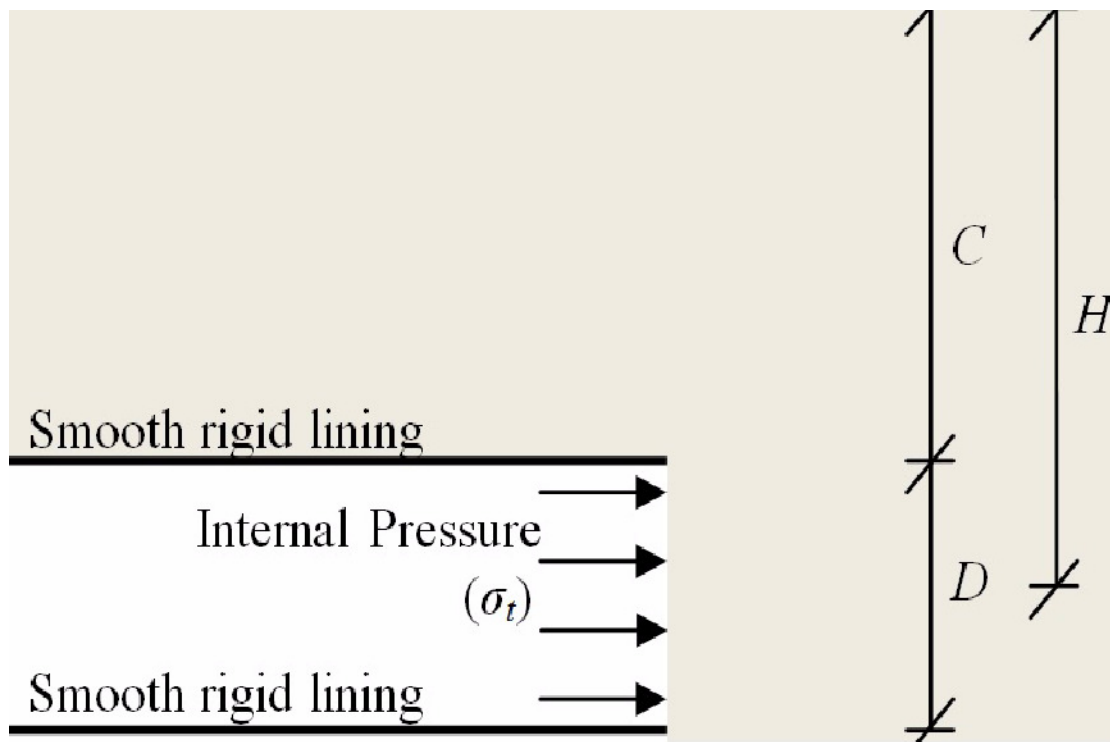


Figure 5-1. Ideal model of system

The system has many assumptions: Mohr-Coulomb failure criteria, plan strain, the tunnel is rigid, and the soil is homogeneous.

5.2.2 Setup and Parameters

The script being used to model this system has been written by Dr Jim Shiau and has been used in Shiau and Kemp (2013). The upper section of the script is below in figure 5-2. This is the section where the relevant parameters can be edited before calling it in *FLAC*.

```
; -----Developed by Dr. Jim Shiau, PhD(Newcastle)
; -----@ University of Southern Queensland, Toowoomba, QLD, 4350, Australia
new
set echo on
set log on
set plot emf
config extra=10;
set overwrite on
set replot on; "off" to add to the existing plot
def para_meter
;-----;CHANGE the following parameters to suit your need;-----;
; -----set up all the parameters of the model
; -----This is the place you can change problem geometry
; -----and material property
    pathname = 'C:\sand\medium\2' ; files will be saved here!!
    save_or_not = 'YES' ; "YES" - save all files (*.sav and *.emf)

    start_from_p = 0 ; increment start from ??? %
    end_at_p = 100 ; only save at ??? % relaxation

    C = 12 ; Height of overburden soil
    D = 6 ; Diameter of the tunnel in metres

    SOIL_DEN = 1800 ; soil density
    SOIL_COH = 0 ; A small 5 Pa to improve numerical stability
    SOIL_FRI = 35 ; zero for clay
    SOIL_DIL = 10 ; ** watch this value very carefully**
    SOIL_TENS = 10e10 ; very limited soil tension(N/m2, Pa)
    SOIL_Young = 50E6 ; Youngs Modulus
    SOIL_poisson = 0.3 ; Poisson's ratio

    Set_grav = 1*9.81 ; centrifuge model - more g
; -----surface pressure set to zero in most cases (in pascal, N/m2)-----
    sigma_s = 0 ; For soft cases, better set sigma_s=0
; -----For strong cases, non-zero sigma_s is required to fail the soil.
    No_step= 5000 ; no of steppings for each relaxation
    No_relax = 11 ; e.g. 21, 31, 51,101 ... etc
    XElementsize = 0.5 ; element size;divide equally with B & H
    YElementsize = 0.5 ; element size;divide equally with B & H
;-----;CHANGE the above parameters to suit your need;-----;
end
```

Figure 5-2. Screenshot of a portion of the FLAC script being used

The soil density and friction angle being used are from the results obtained during the physical modelling. Of course, cohesion is zero as the material in question is dry sand. The dilation angle is a property that describes the volume change of the material when it is disturbed, for dry uncompressed sand, usually it is set to approximately one third of the friction angle (Bolton, 1986). C and D allow control of the C/D ratio, for this project, D was set to six, and therefore C was set to 12, 18, 24, 30, 36, and 42 for each of the six different cases. These parameters control the material properties, and the basic geometry of the system.

The other parameters of interest which control accuracy and precision are the number of steps per relaxation, number of relaxation stages, and the mesh size given by XElementSize and YElementSize. The first of these controls the number of steppings for each stage, it was set to 5000 based on advice from the author of the script. The number of relaxation stages controls how many stress relaxation steps there will be, for example setting it to 21 would result in relaxation stages with stress relaxations of 5% each time: 100%, 95%, 90% etc.. This has been set to 11, which means relaxation decrements of 10% each stage. Mesh size controls the size of the elements in the model. Setting the mesh parameters to 1.0 would be quite a coarse mesh, 0.5 a medium mesh, and 0.1 would be a very fine mesh. Of course setting it lower results in better accuracy, but increased computing time. A typical mesh generated by this script is contained below in figure 5-3.

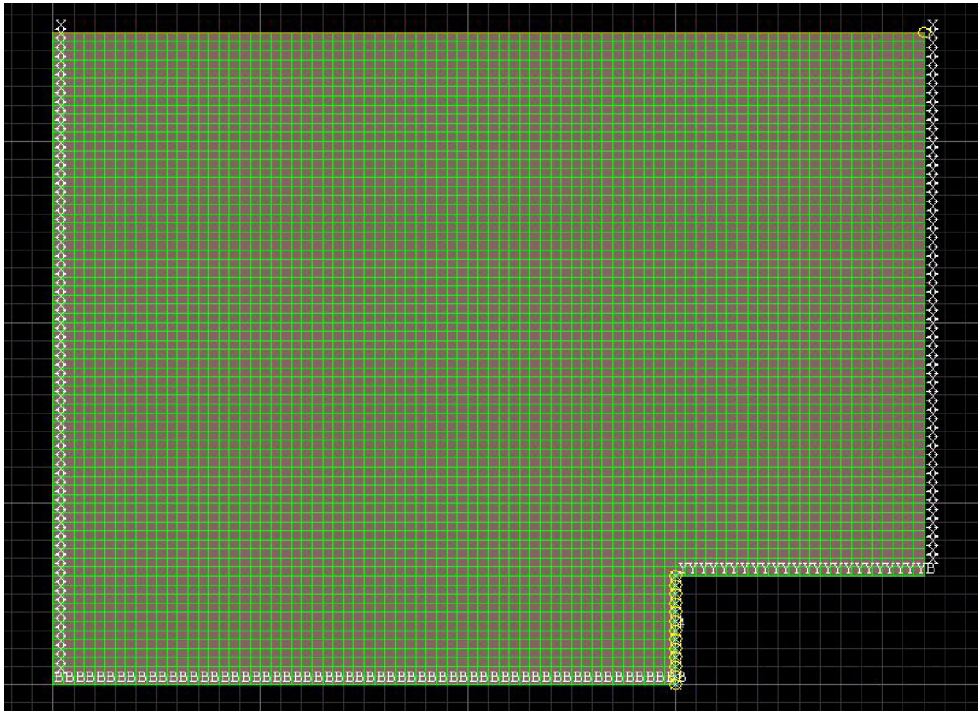


Figure 5-3. Typical mesh in FLAC

In this project, the medium mesh was used. This gave good results with a computing time of about 10 minutes. A trial using the fine mesh early in the project needed about 90 minutes, and gave results that weren't significantly different. Therefore, the medium mesh seems an optimal selection of accuracy and computing time.

5.3 Results

After the script has been configured appropriately, it is called within *FLAC* and it is executed. The script itself exports several graphs of interest by default, but others require extracting the data out of the results files manually. One such graph is shown below in figure 5-4, which shows the relationship between applied heading pressure and the displacement of the heading. It can be seen that the heading pressure in all cases seems to converge upon one common residual value, the minimum support pressure (Kirsch, 2010), below which, total collapse occurs.

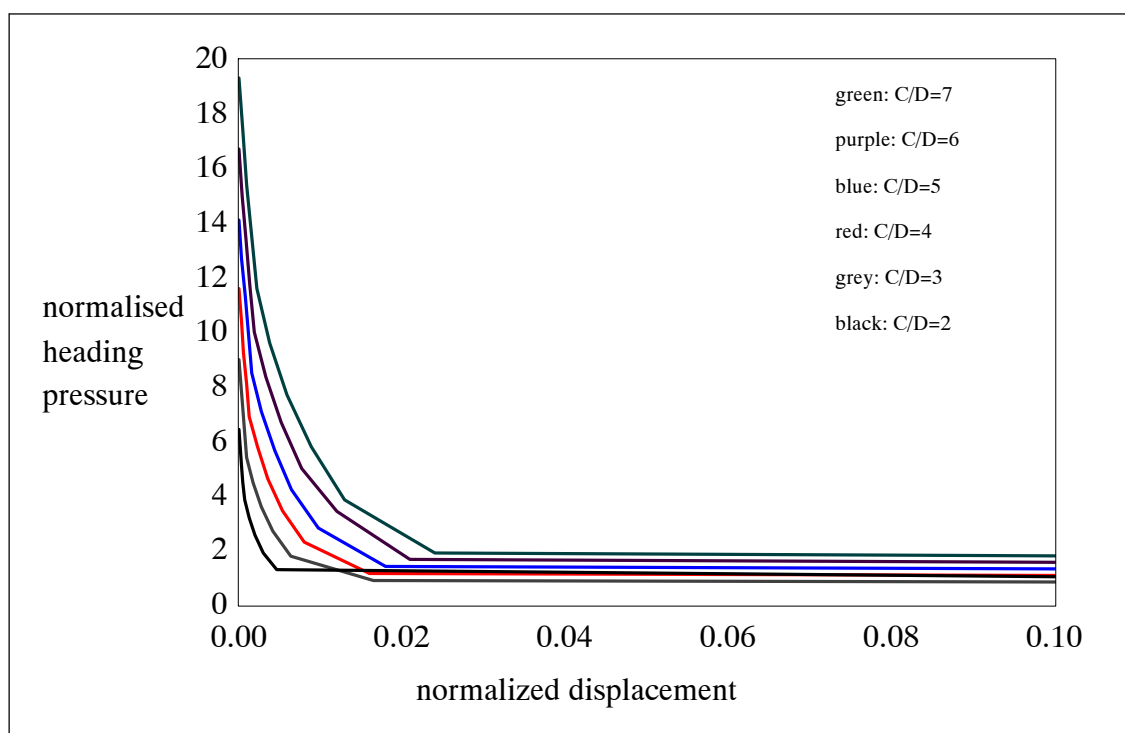


Figure 5-4. Heading pressure and displacement for the six C/D cases

When the program begins a new relaxation stage, the unbalanced forces is quite large as the finite difference method hasn't yet converged on the solution. When total collapse occurs in the tunnel, the program never converges on the solution, and this causes a spike in the history plot of unbalanced forces, as shown below in figure 5-5. In this case the spike occurs in the last stage, between 90% and 100% relaxation. If the history plots for all of the cases are studied, it is seen that the observable failure point occurs earlier for lower C/D and later for higher C/D. The best explanation for this is soil arching, which becomes the dominant stress in the soil at higher C/D's.

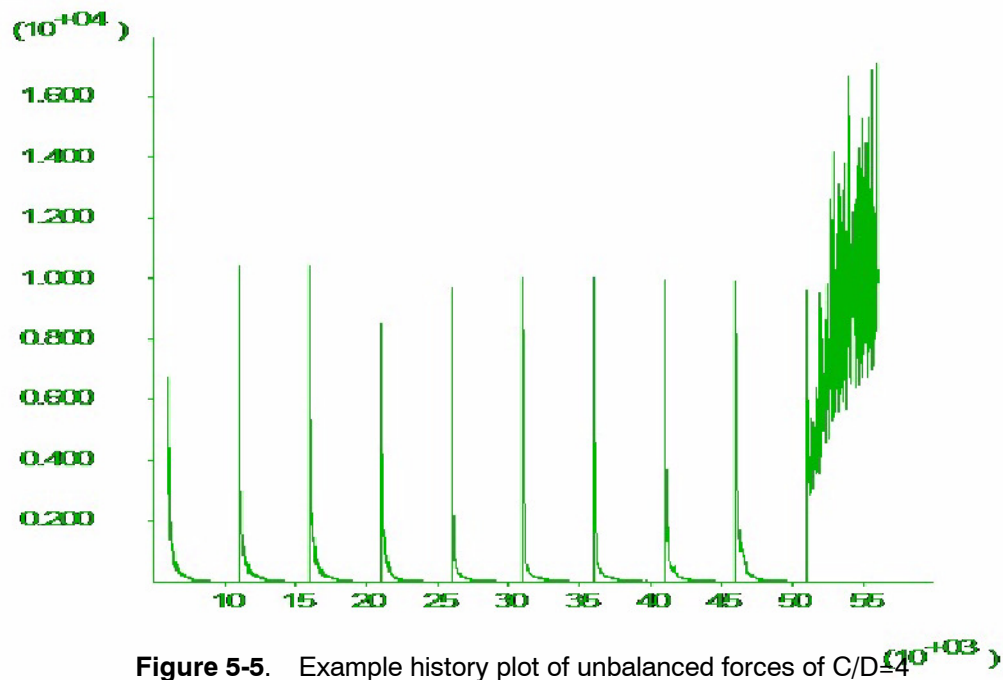


Figure 5-5. Example history plot of unbalanced forces of C/D=4

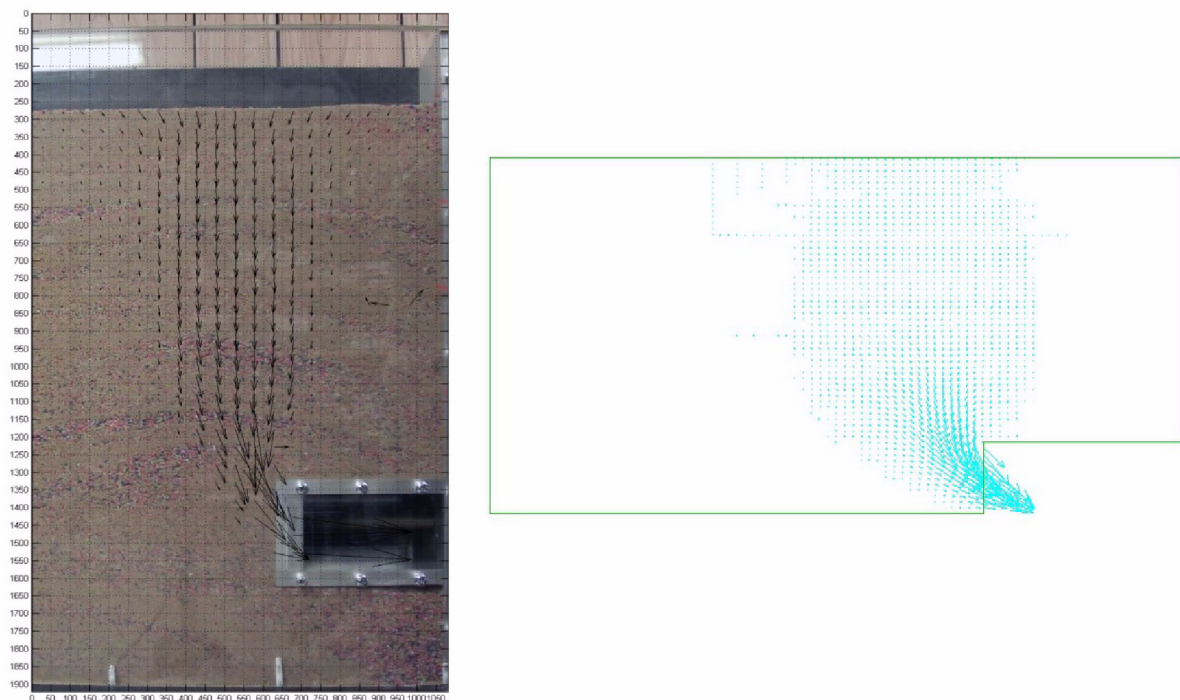


Figure 5-6. Comparison of PIV plot and FLAC velocity plot in the C/D=4 case

Figure 5-6 is a comparison between the PIV vector plot and the FLAC velocity plot for the C/D=4 case. This just shows a fairly nice correlation between the two, and it is seen that the shape of the failure chimney in the two pictures is quite similar. Figure 5-7 below shows something similar, but compares the PIV plot with a strain rate plot from FLAC, which

shows where the soil has sheared. The failure plane seems to be fairly comparable with where the soil has moved in the PIV plot.

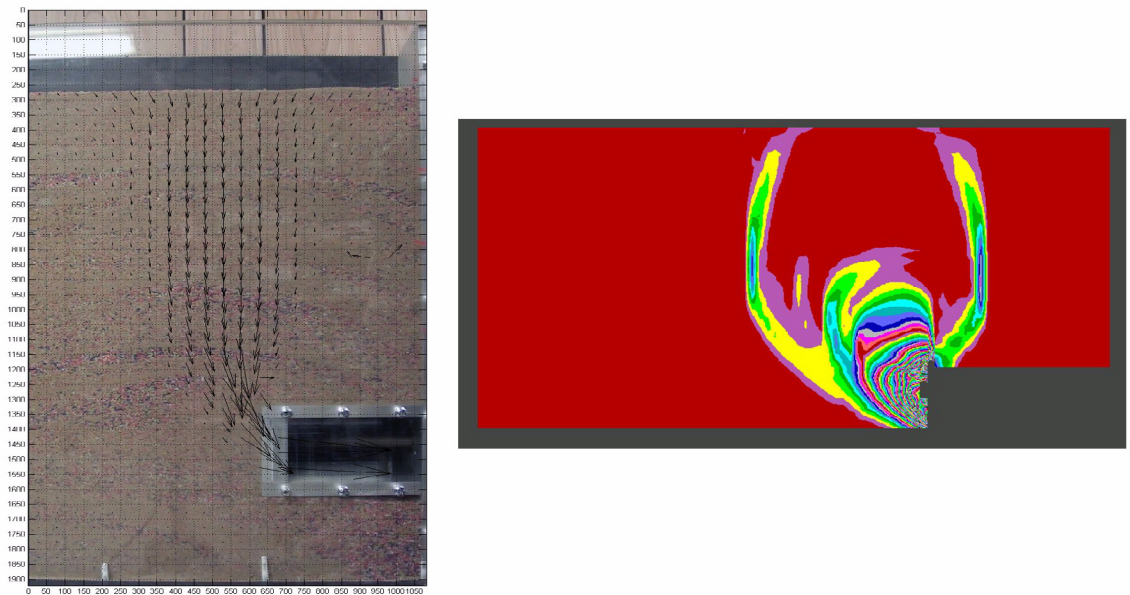


Figure 5-7. Comparison of PIV plot and FLAC strain rate plot for the $C/D=4$ case.

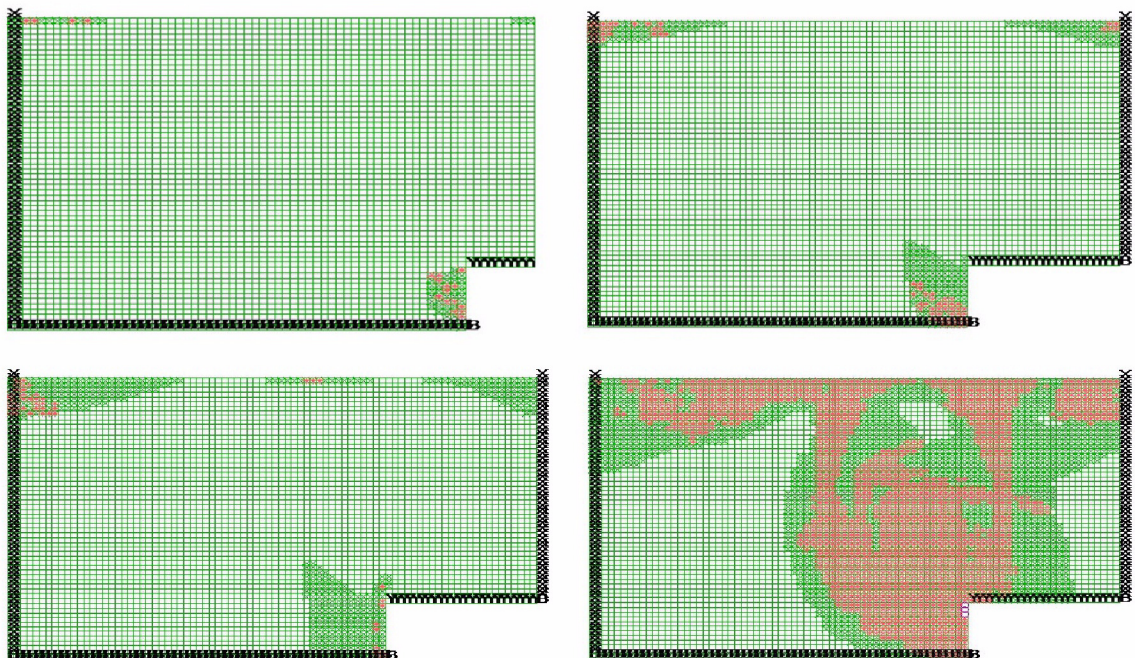


Figure 5-8. Failure plots showing the failure pattern (showing 50%, 80%, 90%, 100% relaxation)

Figure 5-8 shows the failure plots of the $C/D=4$ case at 50%, 80%, 90%, and 100% relaxation. This shows similar findings to an analysis in the PIV chapter and also further agrees with comments made in a paper by Chen et al (2013) that the failure happens in

distinct stages: first a local failure, and then the global collapse occurs when heading pressure is lower than the minimum residual stress.

5.4 Conclusions and Recommendations

An outline of the setup of the model has been given. An introduction to the program script with some more detailed discussion on the more important input parameters. The program has then been run over the six C/D cases using the specified values. Results have been given with some discussion and comparison to earlier parts of the research and other researchers results.

The results seem to correlate quite nicely with particle image velocimetry and the physical modelling completed earlier in this project. Some agreement with papers by Kirsch and Chen et al as also been attained. From this, it can be concluded that the model seems to model soil response to tunnel instability very well.

Because of the limitations with the physical modelling, the comparisons you can draw are limited to qualitative observations only. Upgrading that equipment would allow much better analysis, and would allow better validation of the numerical modelling. There are also some specific improvements that could be made for future projects and research using this script. Namely, using more relaxation stages, would mean that the exact percent relaxation where failure occurred could be identified. As well as this using a finer mesh would give more accurate results.

Conclusions



6.1 Summary

This research paper has investigated tunnel instability in sand with varying overburden (C/D) ratios, using physical modelling with small scale 1g tanks, particle image velocimetry to visualise the planar soil movement, and numerical modelling using FLAC. Using these methods, the behaviour and magnitude of the failure mechanism was investigated. Some key conclusions were:

1. The settlement zone upon heading failure appears to become flatter and wider with increasing C/D. The position of the observed settlement maximum with respect to the heading appears to gradually increase, but by a smaller margin each time. This was attributed to the arching phenomenon present in soils, that acts to redistribute vertical stresses around an opening.
2. Using the footage of the physical modelling, a particle image velocimetry analysis can be undertaken. Using this, the aforementioned settlement characteristics with respect to C/D can be qualitatively verified. It can also be used investigate the stages of failure that the soil goes through as the heading is retracted. It is concluded that the method appears to be two staged, a local then a global failure, which is in agreement with Chen et al (2013).
3. *FLAC* has been used to simulate the same scenarios in the physical modelling. The script that was utilized, uses stress relaxation techniques, whereby a percentage of the initial heading pressure is released in each successive stage. To do the analysis, the soil properties were taken from the physical modelling, and the mesh characteristics were chosen based on optimising computing and accuracy, as well as advice from the author of the script. The results from this analysis further verify some of the conclusions made in previous chapters. Namely, that arching becomes dominant at high overburden ratios, the failure mechanism

is two-staged. The correlation in the failure chimney shapes between the *FLAC* modelling and the physical modelling is also very similar, which would indicate that the script used models the soil response to this particular stimulus accurately.

6.2 Future Work and closing comments

Future work on modelling tunnel stability would require upgrading the small scale models so that they could measure heading pressure against heading displacement. The PIV needs to be done with a higher resolution camera and needs to be calibrated such that it can be used to calculate strain rates across the interrogation zone. Lastly, the *FLAC* modelling needs more relaxation steps and a finer mesh, which would yield greater accuracy and precision. Doing these things would allow quantitative comparison across the three methods, which would be significantly better.

The worldwide demand for tunnels has been increasing over the last few years because of traffic issues in built-up areas, and the modernization of third world countries, such as China. Being able to complete in a smaller timeframe, for less money, and with less risk of disaster is very desirable. Because of this, tunneling is emerging as one of the biggest areas of geotechnical research.

Possible areas of interest are twin tunnels, layered soils with water table, effects of tunneling near a slope, 3D modelling, and so on. The sheer amount of variables and possibilities involved with tunneling, whether that's with the material or with tunnel geometry means that having a single design tool to estimate required heading pressure in a tunnel for every situation is unlikely. This means that there will always need to be tunneling research done for particular scenarios.

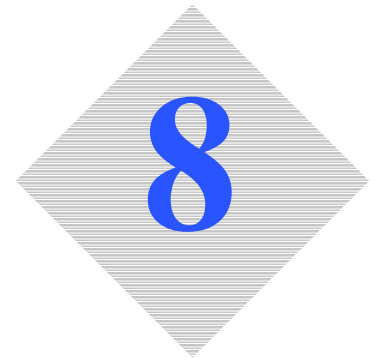
References



- Adrian, R.J. 2005. *Twenty Years of Particle Image Velocimetry*. Experiments In Fluids vol. 39, no. 2, pp 159-169, viewed 15 July 2013.
- Ahmed, M and Iskander, M. 2012. *Evaluation of tunnel face stability by transparent soil models*. Tunnelling and Underground Space Technology 27 (2012) 101-110
- Anagnostou, G. 2012. *The contribution of horizontal arching to tunnel face stability*. ernst and Sohn-Geotechnical 35 (2012), volume 1
- Andrawes, K. Z. & Butterfield, R. (1973). The measurement of planar displacements of sand grains. Geotechnique 23, No. 5, 571-576.
- Atkinson JH, Potts DM. 1977. *Stability of a shallow circular tunnel in cohesionless soils*. Géotechnique 1977;27(2):203-215.
- Butterfield, R., Harkness, R. M. & Andrawes, K. Z. 1970. *A stereo-photogrammetric technique for measuring displacement fields*. Geotechnique 20, No. 3, 308-314.
- Chambon P, Corté JF. 1994. *Shallow tunnels in cohesionless soil: stability of tunnel face*. J Geotech Eng 1994;120(7):1148-1164.
- Chehade, F and Shahrour, I. 2008. *Numerical analysis of the interaction between twin-tunnels: Influence of the relative position and construction procedure*. Tunnelling and Underground Space Technology 23 (2008) 210-214
- Chen, R, Tang, L, Ling, D, and Chen, Y. 2011. *Face stability analysis of shallow shield tunnels in dry sandy ground using the discrete element method*. Computers and Geotechnics 38 (2011) 187-195
- Chen, R, Li, J, Kong, L, and Tang, L. 2013. *Experimental study on face instability of shield tunnel in sand*. Tunnelling and Underground Space Technology 33 (2013) 12-21
- Jebelli, J, Meguid, M, and Sedghinejad. 2010. *Excavation failure during micro-tunneling in fine sands: A case study*. Tunnelling and Underground Space Technology 25 (2010) 811-818

-
- Kirsch A. 2010. *Experimental investigation of the face stability of shallow tunnels in sand*. Acta Geotech 2010;5: 43–62.
- Koliji, A. 2013. *Direct Shear test*. viewed 20th August 2013.
<<http://www.geotechdata.info/geotest/direct-shear-test.html>>
- Leca E, Dormieux L. 1990. *Upper and lower bound solutions for the face stability of shallow circular tunnels in frictional material*. Géotechnique 1990;40(4): 581–606.
- Messerli, J, Pimentel, E, and Anagnostou, G. 2010. *Experimental study into tunnel face collapse in sand*. Physical Modelling in Geotechnics – Springman, Laue & Seward (eds)
- Michalowski, R. 2003. *Arching in Granular Soils*. ASCE – Geomechanics: testing, modeling, and simulation
- Mollon, G, Dias, D, and Soubra, A. 2009. *Probabilistic Analysis and Design of Circular Tunnels against Face Stability*. ASCE – International journal of geomechanics (Nov/Dec 2009)
- Ohta, T, and Kiya, H. 2001. *Experimental Study and Numerical Analysis on Stability of Tunnel Face in Sandy Ground*. QR of RTRI, Vol 42, No. 3, Sep. 2001
- Peck, R.B., 1969. *Deep Excavations and Tunneling in Soft Ground*. In: Proceedings of the 7th International Conference on Soil Mechanics and Foundation Engineering, Mexico City, State-of-the-art Volume, pp. 225–290.
- Phillips, R. 1991. *Film measurement machine user manual*. Cambridge University Technical Report, CUED/D-Soils/TR 246.
- Prasad, A. 2000. *Particle Image Velocimetry*. Current Science Vol. 79, No. 1
- Sadrekarimi, J, and Abbasnejad, A. 2008. *An Experimental Investigation into the Arching of Sand*. IJE Transactions B: Applications, Vol. 21, No. 4, December 2008
- Vardoulakis, P., Stavropoulou, M. & Exadaktylos, G. 2009. *Sandbox modeling of the shallow tunnel face collapse*. Rivista di Geotecnica 1/2009, 9–21.
- Vennermann, P. 2013. *Introduction to JPIV*. viewed 15th July 2013.
<<http://www.jpiv.vennermann-online.de/introduction.html>>
- Vermeer PA, Ruse NM, Marcher T. *Tunnel heading stability in drained ground*. Felsbau 2002;20(6):8–18.
- White D.J, Take W.A & Bolton M.D. 2003. *Soil deformation measurement using particle image velocimetry (PIV) and photogrammetry*. Geotechnique 53, No. 7, 619–631
- Wong, K, Ng, C, Chen, Y, and Bian, X. *Centrifuge and numerical investigation of passive failure of tunnel face in sand*. Tunnelling and Underground Space Technology 28 (2012) 297–303

Appendices



8.1 Appendix A - Project Specification

University of Southern Queensland
FACULTY OF ENGINEERING AND SURVEYING
ENG4111/2 Research Project

PROJECT SPECIFICATION

FOR:	Mathew Steven Sams
TOPIC:	Numerical and Physical Modelling of a 2D Tunnel Heading at Collapse
SUPERVISOR:	Dr Jim Shiau
ENROLMENT:	ENG4111 - S1, 2013 ENG4112 - S2, 2013

PROJECT AIM:

To investigate the failure mechanism of a tunnel heading in sand at various depths using physical models with Particle Image Velocimetry analysis (PIV), and also numerical modelling with FLAC.

PROGRAMME:

1. Gather other research that has been completed on this and related topics. Study these papers, to gain insights into their methods.
2. Design and modify the physical models such that the depth and clear viewing window requirements are met, using previous research for guidance.
3. Perform the experiments with the physical models while capturing on a High definition camera. Attain the characteristics of the sand at the same time.

4. Carry out the PIV analysis and the numerical modelling (FLAC) analysis using the attained sand characteristics.
5. Analyze the data obtained and present findings and conclusions in a relevant manner.

As time permits:

6. 3D modelling of the tunnel heading collapse
7. Modelling of twin tunnel collapse

8.2 Appendix B - Display script for PIV results

Custom output display script: displays displacement vectors across the entire image sample and displays on the first image:

```
%%Mathew Sams
%%PIV output script

clc

img=imread('5_000.jpg');
min_x=0;
max_x=1080;
min_y=0;
max_y=1920;

x=50; %pixel box size
n=36; %number of images in sample

for i=1:n;
    qq(data,1,i,1);
    set(gcf,'Position',get(0,'Screensize'));
    set(gca,'xtick',0:x:max_x), set(gca,'ytick',0:x:max_y)
    grid on

    %M(i)=getframe;
end
pause(2)

imagesc([min_x max_x], [min_y max_y], img);
hold on
qq(data,1,n,1);
set(gcf,'Position',get(0,'Screensize'));
set(gca,'xtick',0:x:max_x), set(gca,'ytick',0:x:max_y);
grid on

%numtimes=1;
%fps=4;

%movie(M,numtimes,fps);
```


8.3 Extra Reference Material

Included on the cd is the video footage from which the frames were extracted. These have been included for the purpose of providing original data. These can be found in the folder “Extra Reference Material”.